Top Heterocycl Chem (2021) 58: 175–208
https://doi.org/10.1007/7081_2021_53

Published online: 14 February 2021

Siderophores from Fish Pathogenic Bacteria

Carlos Jiménez

Contents

Abstract Aquaculture is an important food source worldwide but one of its main problems is the spread of infectious diseases caused by Gram-negative pathogenic bacteria that results in considerable economic losses. Since siderophores, low molecular weight organic compounds involved in the iron-uptake mechanisms of the bacteria, are critical for the growth and virulence of the producer pathogens, the bacterial iron acquisition systems are promising targets for the design of new antimicrobial strategies. In this chapter, the current chemical knowledge of the siderophores involved in the iron-uptake mechanisms of Gram-negative pathogenic bacteria *Vibrio anguillarum*, *Photobacterium damselae* subsp. *piscicida*, and *Aeromonas salmonicida* subsp. s*almonicida,* responsible for the main fish infectious diseases Vibriosis, photobacteriosis, and furunculosis, respectively, is summarized. The isolation, structural elucidation, and the chemical synthesis of the siderophores biosynthesized from those bacteria are displayed. Their involvement in the iron-uptake mechanisms, virulence importance, and the application in the development of new strategies to fight against the infectious diseases will be also discussed.

C. Jiménez (✉)
Departmento de Química, Facultade de Ciencias e Centro de Investigacións Científicas Avanzadas (CICA), AE CICA-INIBIC, Universidade da Coruña, A Coruña, Spain
e-mail: carlos.jimenez@udc.es

Keywords *Aeromonas* · Fish diseases · Iron acquisition · Pathogenic bacteria · *Photobacterium* · Siderophore synthesis · Siderophores · *Vibrio*

1 Introduction

The need for a safe, reliable, and economic supply of food to feed the high increase of human population is transforming aquaculture as an important food source worldwide. According to the Food and Agriculture Organization (FAO) of the United Nations, global fish consumption (from wild fishing and aquaculture) grew at an average of 3.1% yearly from 1961 to 2017, which is a rate almost twice that of the 1.6% annual world population increase. While wild fishing production has stabilized in the last 20 years, global aquaculture production increased more than five times in the last three decades (from 14.9 million tonnes in the period 1986/1995 to 82.1 million tonnes in 2018). Right now, more than 50% of fish for human consumption comes from aquaculture [1].

However, the production intensification increases the likelihood of pathogen outbreaks and the emergence of several infectious diseases which are causing severe economic losses in aquaculture (Fig. 1a) [2]. The extensive use of antibiotics has contributed to the spread of antimicrobial resistance (AMR), which has become a global health emergency. Moreover, fish are reservoirs of zoonotic pathogens such as *Aeromonas hydrophila* and *Photobacterium damselae* that can infect not only the animal host but also humans who are in contact with the aquaculture facility and via foodborne infections [3]. For all these reasons, the search for new strategies to prevent and control diseases in aquatic species is urgently needed. It is one of the main research objectives within the field of health in the next decade.

For most bacteria, iron uptake ability during the naturally iron-limited conditions of an infection is a key virulence factor essential for multiplication within the host. Iron is a crucial nutrient in virtually all living organisms because it is needed in many metabolic processes, catalyzing a wide variety of indispensable enzymatic reactions. The wide range of properties of iron and its abundance, being the fourth most abundant element in the Earth's crust, could explain why early microorganisms, from the beginning of evolution, used this element to develop their metabolic processes in an oxygen-poor atmosphere. However, when the atmosphere became rich in oxygen, ferrous iron was oxidized to ferric ion which precipitates to form ferric hydroxide which is highly insoluble at physiological pH. Since then, the bioavailability of free ion became very low and the iron acquisition uptake mechanisms to combat the extremely low iron availability became an indispensable process for most living organisms [4]. Now, a high competition for this scarce iron is taking place and so, iron sequestration systems have been identified as important virulence mechanisms in several pathogenic bacteria. In fact, potential hosts keep the level of free iron inside the body to a minimum as a defense mechanism.

One of the major strategies used by bacteria and fungi entailed the use of siderophores, a Greek term that means iron carriers. These are low molecular weight organic compounds that have extremely high affinity for ferric iron [5]. Thus, bacteria and fungi excrete "endogenous" siderophores into the culture medium

A)

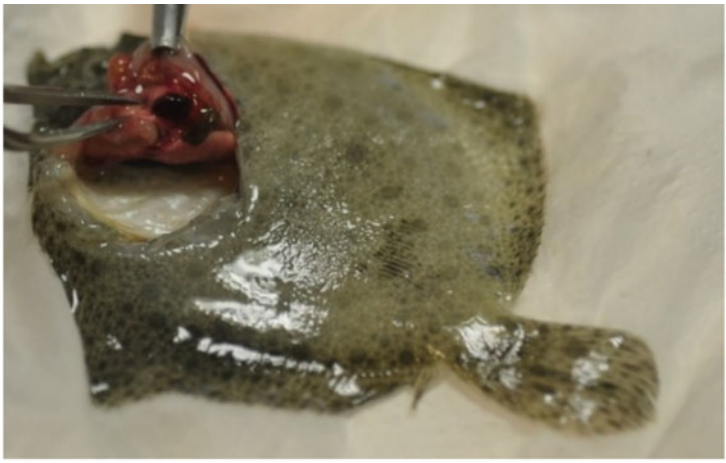

B)

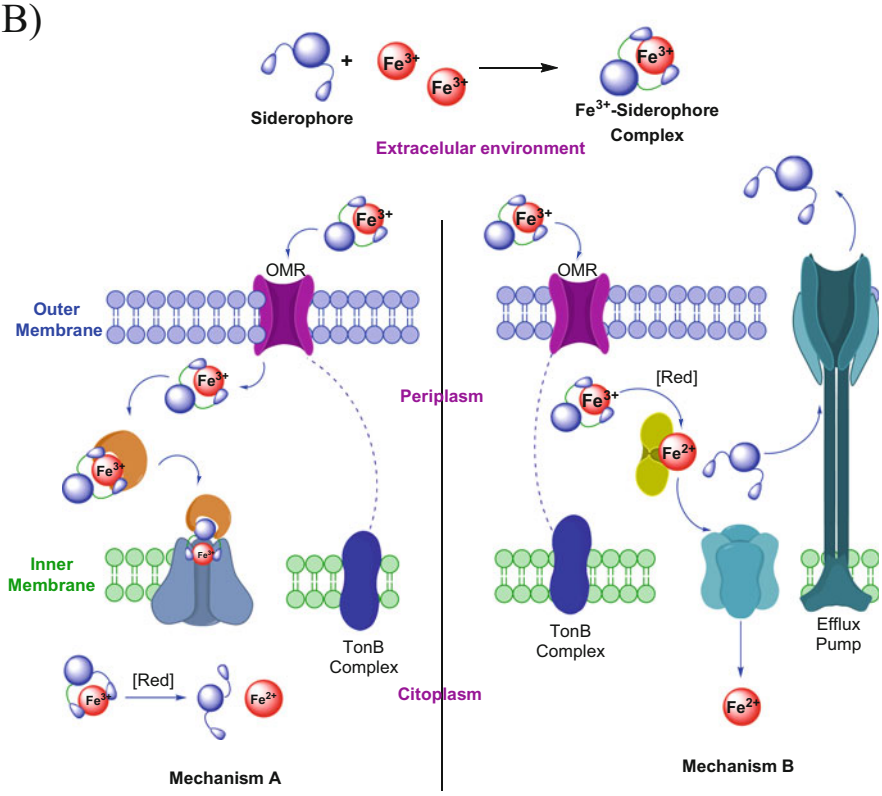

Fig. 1 (**a**) Turbot infected with photobacterioisis. (**b**) General iron uptake mechanisms in Gram-negative bacteria

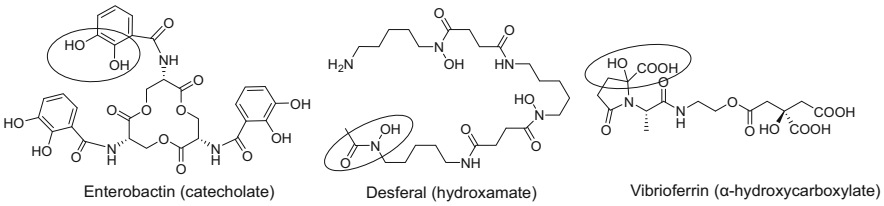

Fig. 2 Examples of the main types of microbial siderophores

where they are able to solubilize Fe (III) from its hydroxide or they can efficiently sequester the iron bound by transferrins and other iron-holding proteins within the host. Once siderophores are synthesized and secreted outside the bacterial cells, they bind Fe^{3+} ions to form a ferric-siderophore complex which is then internalized by the appropriate transport mechanism. In Gram-negative bacteria, ferric-siderophore complexes are recognized by specific outer membrane receptors (OMR). These proteins trigger the transport system across the outer and inner membranes, thus permitting the delivery of iron into the cells by an energy-dependent system. The components of such systems include a specific TonB-dependent ferric-siderophore transporter (TBDT) protein located in the outer membrane that is energized through the TonB system. The TBDT protein is coupled to an ABC transporter that catalyzes the final stages of ferric-siderophore transport through the cytoplasmic membrane from the periplasm to the cytosol [6]. Finally, the reduction of Fe^{3+} to Fe^{2+} by microbial-mediated processes is the most common mechanism for the release of the iron inside the cell (Fig. 1b) [7]. Additionally, some microorganisms are able to use the xenosiderophores, siderophores biosynthesized by other organisms, due to the presence of OMR that can recognize a wide spectrum of siderophores with the same type of chelating units.

On the basis of the bidentate groups involved in iron (III) binding, siderophores can be classified into four main classes: phenolates or catecholates, hydroxamates, α-hydroxycarboxylates, and mixtures with these functionalities (Fig. 2) [5].

Iron restriction is an important host defense strategy; thus, successful pathogens must possess mechanisms to acquire iron from host sources in order to cause disease. During infection, a fierce battle of iron acquisition occurs between the host and bacterial pathogens. For that reason, siderophores are not only crucial in bacteria iron metabolism but also are key factors in the virulence to enhance the infection disease. In this way, the iron-uptake mechanism mediated by siderophores along with their structures provides an ideal target for therapeutic applications [4]. Indeed, the natural siderophore "desferal," produced by *Streptomyces pilosus*, is used in clinics for the removal of excess iron in human blood, a disease known as thalassemia [8]. But one of the most promising applications of siderophores is for the development of new antibacterial treatments based on iron acquisition, such as novel antimicrobials and vaccines. Thus, iron-uptake mechanisms mediated by siderophores are providing the basis for the development of new antibacterial treatments: by the Trojan horse Strategy where the siderophore is coupled to a known antibiotic in order to overcome the permeability barrier of the Gram-negative outer membrane that uses a specific

siderophore route of entry into the cell. The natural siderophore-antibiotic conjugates (sideromycins), such as albomycins and salmycins, inspired this methodology [9]. This approach seeks to avoid microbial resistance, thus enhancing sensitivity and specificity. In fact, the catechol based-siderophore cefiderocol (Fetcroja®) is the first siderophore-drug conjugate approved by the U.S. Federal Drug Administration (FDA) [10] and the European Medicines Agency (EMA) [11]. Other applications imply the inhibition of biosynthesis of siderophore and the development of vaccines [4].

Vibriosis, photobacteriosis, and furunculosis, caused by Gram-negative marine bacteria, constitute the main infectious diseases in aquaculture [12]. In the present chapter, studies of the siderophores from the fish Gram-negative pathogenic bacteria involved in those infectious diseases and its application in fish farming will be presented. Special attention will be paid to the isolation methodology used, the synthesis of natural siderophores and their derivatives, the establishment of some Structure Activity Relationship (SAR), the biosynthetic proposals and the OMR involved.

2 Vibriosis by *Vibrio anguillarum*

Vibriosis is a group of diseases that cause a serious hemorrhagic septicemia associated with both wild and farmed marine fishes. This leads to severe economic losses in the aquaculture industry worldwide. Different Gram-negative bacterial species, mainly classified into the *Vibrio* genus, belonging to the family of Vibrionaceae are responsible for this infection [13]. The bacillus *V. anguillarum* is considered the etiological agent of classical vibriosis, being the most common and also the most extensively studied Vibrionaceae species. Its virulence in marine settings was reported as early as 1718 along the coastline of continental Europe and was referenced on record as the red disease in eel (*Anguilla anguilla*) in 1893, serving as the root of the name *anguillarum*. By 1970, it was known to have devastating effects on several marine organisms (cod, eel, finnock, oyster, salmon, trout, etc.) and now has a wide geographical distribution and host range. *V. anguillarum* is pathogenic to a variety of crustaceans, bivalves and mainly to warm- and cold-water fish of economic importance, including Pacific and Atlantic salmon, rainbow trout, turbot, sea brass, sea bream, among others, accounting for more than 90 susceptible aquatic species in at least 28 different countries [14]. A total of 23 different O serotypes of *V. anguillarum* isolates have been recognized. Among them, O1 and O2 are the main ones implicated in the infections, although serotype O3, and to a lesser extent O4 and O5, have increasing importance in vibriosis outbreaks in specific geographic areas [15]. The remaining serotypes are considered to be environmental strains and only on rare occasions are isolated as responsible for vibriosis in fish [16].

For a long time, just two different siderophore-mediated systems were described in *V. anguillarum* strains belonging to serotypes O1 and O2, the anguibactin (Ang, **1**) and the vanchrobactin (Vcb, **2**). More recently, a third one was reported,

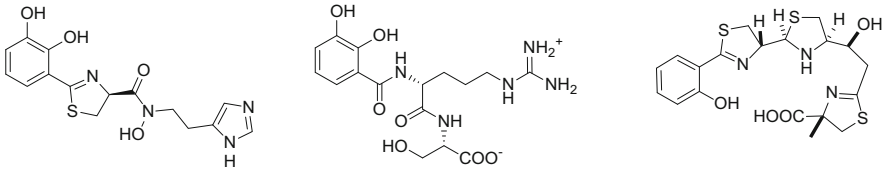

Fig. 3 Structure of the siderophores biosynthetized by *V. anguillarum*

piscibactin (Pcb, **3**), which turned out to be one of the most important virulence factors for this bacterium (Fig. 3). Additionally, *V. anguillarum* can also use xenosiderophores as iron sources, like enterobactin, ferrichrome or rhodotorulic acid.

2.1 Anguibactin Iron-Uptake System

The first siderophore-mediated system described in this bacterium, called anguibactin system, was found in pathogenic strains of serotype O1, which bears the 65 kb pJM1 plasmid that harbors the genes for the biosynthetic machinery and utilization of the siderophore anguibactin (Ang, **1**).

Ang (**1**) was purified from its supernatants of iron-deficient cultures by adsorption onto an XAD-7 resin and subsequent gel filtration on a Sephadex LH-20 column and reported in 1986 [17]. Three years later, its hybrid structure between a catechol and a hydroxamate type of siderophore was determined by ^{1}H- and ^{13}C-NMR spectral analysis of its Ga(III)-complex, FAB-MS, chemical degradation, and single-crystal X-ray diffraction studies of its anhydro derivative, anhydroanguibactin (**4**) [18]. The crystal structure of the Ga(III)-complex of anguibactin was reported in 1998 [19]. However, the absolute configuration of the cysteine moiety in Ang (**1**) was not determined at that time.

The structure of Ang (**1**) is similar to that of preacinetobactin (PreAcb, **5**), which contains instead an oxazoline ring. PreAcb (**5**) is the precursor of acinetobactin (Acb, **6**), the siderophore produced by the Gram-negative pathogen *Acinetobacter baumannii,* which constitutes one of the major health concerns because it is responsible for a large number of hospital-acquired and nosocomial infections and by its increasing development of antimicrobial resistance (Fig. 4) [20].

Since the content of siderophores from marine bacteria is very low and they have potentially valuable applications, the development of chemical synthesis is a crucial step to further study their biological activities, mechanisms, absolute configurations, and/or structure-activity relationships. Furthermore, the synthesis of analogues gives us very important information, for instance, for the preparation of conjugates to be used as biosensors to study these mechanisms [21], for the development of novel therapies against iron-overload related disease [8], for the preparation of new

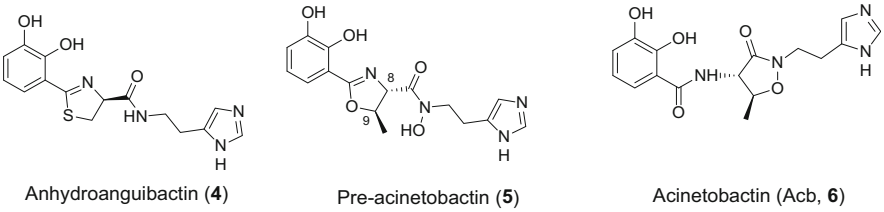

Fig. 4 Similar structures to that of Ang (**1**)

antimicrobial agents that target bacterial pathways for the acquisition of iron [22], for a Trojan horse strategy to develop modified molecules with antimicrobial activity [9], or for the synthesis of bioconjugates of siderophores to be tested as antibacterial vaccines [23].

The total synthesis of Ang (**1**), published by H. J. Kim and co-workers in 2018, started with the preparation of N^{α}-benzyloxyhistamine (**9**) which was obtained from histamine dihydrochloride in three steps following the same procedure employed in the synthesis of Acb (**6**) [24]. The reaction of histamine dihydrochloride with $NaNO_2$ in acid media followed by treatment with $SOCl_2$ gave **7**. Coupling of **7** with *N-tert*-butoxycarbonyl(Boc)-*O*-benzyloxyamine afforded imidazole **9** after deprotection with TFA. In parallel, the thiazoline fragment **12** was obtained by the coupling of aryl nitrile **10**, prepared from *o*-vanillin, with L-cysteine.

Condensation of thiazoline acid **12** with N^{α}-benzyloxyhistamine (**9**) was one of the key steps of the synthesis in order to avoid the epimerization observed at position 8, because the coupling gives a near-racemic mixture. The lack of a substituent at position 9 in Ang (**1**), in relation to that in Pre-acb (**5**), seems to justify that racemization. The presence of an (*R*)-methyl group at C-9 in Pre-acb (**5**) could secure the sterically stable *trans* geometry with the (*S*)-configuration at C-8. The use of **H**exafluorophosphate **A**zabenzotriazole **T**etramethyl **U**ronium (HATU) in dichloromethane with a free amine form of **9** resolved this problem, giving the intermediate **14** with a stereoselective ratio of er = 98:2. The problematic removal of the two ether-type protecting groups present in **14** using boron trichloride (BCl_3) in the final step was solved by the addition of tetrabutylammonium iodide (TBAI), which allowed a clean removal of both benzyl and methyl groups. Using a similar procedure, the anguibactin analogue, 3-deoxyanguibactin (**16**), was also prepared (Scheme 1). The preparation of synthetic siderophore **1** made it possible to determine, by fluorescence titrations, a 2:1 binding stoichiometry between Ang (**1**) and Fe (III) in liquid phase. Furthermore, the iron delivery capability of Ang (**1**) and its thermal stability over PreAcb (**5**) led the authors to propose Ang (**1**) as a competent surrogate siderophore for *Acinetobacter baumannii* that can be useful for the future development of a siderophore-based antibiotic delivery system against that pathogen [25].

Evaluation of cytotoxic effects of Ang (**1**) on P388 murine leukemia cell lines displays an IC_{50} value of <15 μM [26]. Moreover, Ang (**1**) has been patented for performing deferration therapy due to its properties for removing ferric iron from

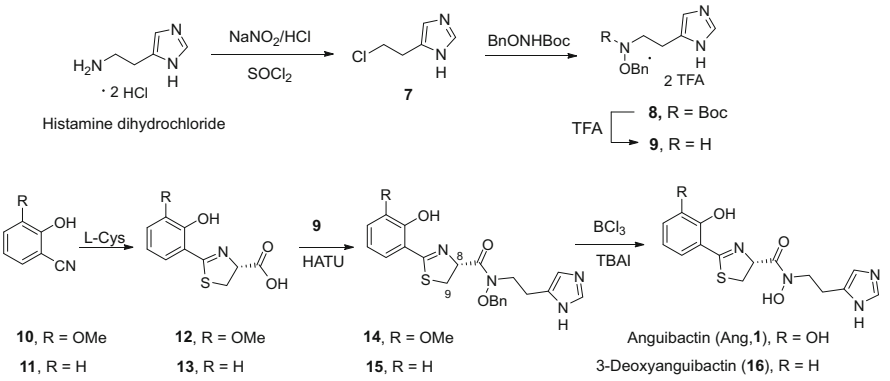

Scheme 1 Synthesis of Ang (**1**) and its analogue 3-deoxyanguibactin (**15**)

aqueous liquids. Among other properties, it was found that Ang (**1**) inhibits iron uptake by living cells, wrests iron from vertebrate tissues, removes iron from other siderophores and ferric hydroxide, and removes ferric iron from aqueous solutions, including cell-culture media [27].

Most biosynthetic genes of Ang (**1**) are located in the pJM1 plasmid and it is accomplished by a complex of non-ribosomal peptide synthetases (NRPS). However, its biosynthesis requires additional chromosomally encoded enzymes that are also involved in the production of Vcb (**2**) as the second siderophore described. The pJM1 plasmid series is present in most *V. anguillarum* O1 strains but is absent in serotype O2. The ferric iron-anguibactin complex is transported by the FatABCD proteins, all encoded by the pJM1 plasmid: the OM receptor FatA, the periplasmic binding protein FatB, and the inner membrane proteins FatC and FatD (ABC transporter) [28].

2.2 *Vanchrobactin Iron-Uptake System*

The second siderophore-mediated iron-uptake system reported in *V. anguillarum* was the vanchrobactin system. Vanchrobactin (Vcb, **2**) is encoded by a gene cluster located in the chromosome that was first found in all serotype O2 strains and some plasmid-less serotype O1 strains. The terms of *V. anguillarum* ("van"), chromosome ("chro") and the suffix "bactin" for chelating agent, were used to name this siderophore as vanchrobactin.

This compound was isolated for the first time from iron-deficient cultures of *V. anguillarum* serotype O2 strain RV22 by using a XAD-7 lipophilic resin, liquid–liquid fractionation, Sephadex LH-20, and RP-HPLC. Its planar structure was established by analysis of its 1D and 2D NMR, IR, UV, and mass spectral data as a dipeptide made up of the amino acids arginine and serine linked to a 2,3-dihydroxybenzoyl moiety [29]. A faster and a more convenient isolation

procedure using Hydrophilic-Lipophilic Balance (HLB) resins followed by HPLC-HRMS analysis was developed and applied in the re-isolation of Vcb (**2**). This method, named as SPE-HLB/HPLC-HRMS, improved not only the efficiency of the isolation methodology but also the isolation time in relation to the existing methods [30].

The absolute configuration of Vcb (**2**) was established by synthesis of three out of four possible stereoisomers using 2,3-dihydroxybenzoic acid (DHBA), L/D-ornithine, and L/D-serine as starting materials and comparison to the natural product. Thus, 2,3-dibenzyloxybenzoic acid (**17**), prepared in three steps from DHBA, was coupled with N^{δ}-Cbz-D-ornithine-OMe (**16a**), obtained in four steps from D-ornithine, or with N^{δ}-Cbz-L-ornithine-OMe (**16b**), prepared from esterification of the commercial N^{δ}-Cbz- L-ornithine, to give acids **18a,b**, respectively, after saponification. Then, *tert*-butyl esters of L/D-serine, synthetized from commercial amino acids, were coupled to acids **18a,b** to afford **19a-c**. Deprotection of the benzyl groups in **19a-c**, followed by introduction of the guanidine functionality and deprotection of the *tert*-butyl group in acid media, yielded three out of the four possible stereoisomers of vanchrobactin. Comparison of the synthetic compounds with the natural sample by achiral HPLC, chiral capillary electrophoresis, along with NMR data, sign and value of the optical rotation allowed to establish the absolute structure of Vcb (**2**) as *N*-[*N*′-(2,3-dihydroxybenzoyl)-D-arginyl]-L-serine (Scheme 2) [31].

Two series of vanchrobactin analogues were synthetized using a similar strategy employed in the total synthesis of Vcb (**2**). The first one where the 2,3-dihydroxybenzoyl moiety is linked to Arg or Orn residues, compounds **20**–**24**, (Scheme 2) and the second series where it was the serine residue which was linked directly to the aromatic moiety, compounds **27**–**29** (Scheme 3).

The synthesized compounds were subjected to the chrome azurol-S (CAS) test and evaluated by growth promotion assay (siderophore activity test) with several bacteria that are well known for their ability to transport and use natural siderophores, specified in brackets: *V. anguillarum* RV22 (serotype O2) (Vcb (**2**) and Pcb (**3**)), *V. anguillarum* 775 (serotype O1) (Ang (**1**)), *Salmonella enterica* enb-1 (enterobactin), *Erwinia chrysanthemi* PPV20 (chrysobactin (**34**)), and *V. alginolyticus* TA15 (vibrioferrin). Most of analogues were positive in the CAS test and showed siderophore activity to both *V. anguillarum* serotypes tested. Although most of them displayed siderophore activity to *S. enterica* and *E. chrysanthemi*, none of them were able to restore the growth of *V. alginolyticus*. These results are in agreement with the catecholate structure of enterobactin and chrysobactin (**34**) and the non catecholate structure of vibrioferrin, an α-hydroxycarboxylate siderophore (Fig. 1). From the results, it was suggested that the aromatic ring in catecholate siderophores is crucial for the binding of the outer membrane receptors. Additionally, the results reveal the lack of stereoisomeric influence of the amino acid scaffold on the siderophore activity in both serotypes of *V. anguillarum*, although some differences can be observed in *E. chrysanthemi* PPV20 and *S. enterica*. This lack of specificity could be an evolutionary adaptation of bacterial pathogens to increase the number of possibilities to obtain iron from the

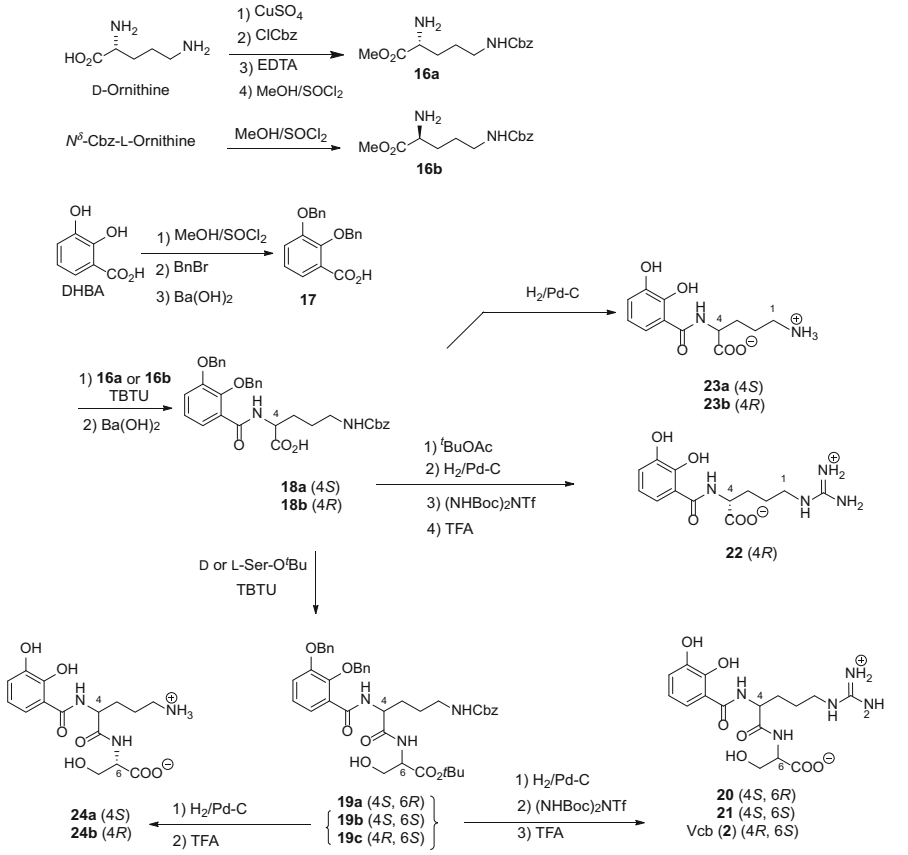

Scheme 2 Synthesis of Vcb (**2**) and its analogues DHBA-Arg/Orn **20**–**24**

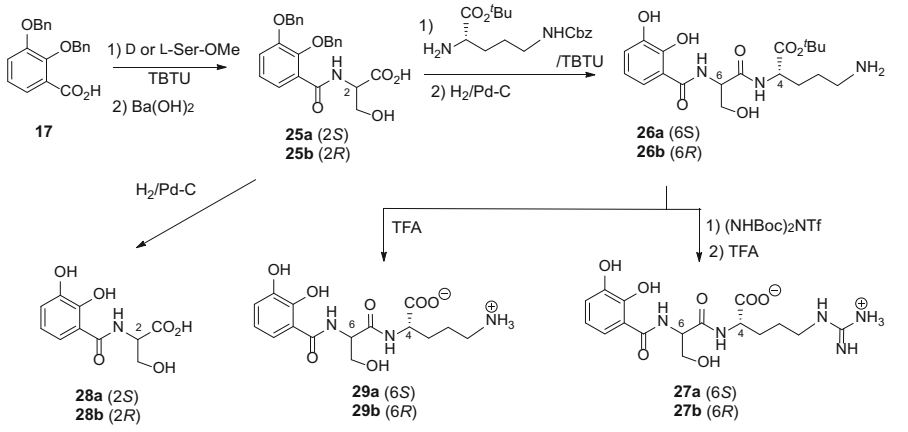

Scheme 3 Synthesis of Vcb analogues DHBA-Ser **27**–**29**

environment. The low specificity of molecular recognition of the recipients of these strains could facilitate the use of those conjugates to be prepared. Analogues having ornithine (**23**–**24**) instead of arginine (**20**–**22**) residue maintain the siderophore activity to *V. anguillarum*, as the Vb analogue DHBA- D-Orn- L-Ser (**24b**), and they are of special interest since these molecules possess an appropriate functionality, an amino group, that can be used as an anchor group to attach it to other bioactive agents. For these reasons, these compounds were considered as potential antibiotic vectors for the delivery of known antibacterial agents via the bacterial iron-uptake systems [32].

Vcb (**2**) is structurally related to chrysobactin (**30**), isolated from the phytopathogenic bacterium *E. chrysanthemi*, which bears a lysine residue instead of arginine. This compound also has the L configuration for the serine residue, while the lysine residue has a D configuration as the arginine in Vcb (**2**) [33]. From an identified species of *Vibrio*, DS40M4 strain, a bis- and triscatechol amide analogues of Vcb (**2**), named divanchrobactin (**31**) and trivanchrobactin (**32**), were isolated. Vcb (**2**) and Ang (**1**) were also isolated from this bacterium and represented the first case that the two siderophores were isolated from the same strain. Their isolation was carried out using Amberlite XAD-2 resins and HPLC. The isolation of **31** and **32** raised the question whether linear trivanchrobactin is the real siderophore or comes from a hypothetical cyclic ester, a cyclic trivanchrobactin product, which was not detected or isolated due to the instability of the cyclic triserine ester or the reactivity of a possible esterase [34]. Curiously, cyclic trichrysobactin, linear trichrysobactin (**33**), and dichrysobactin (**34**) along with the monomeric siderophore unit, chrysobactin (**30**) were isolated from plant pathogen *Dickeya chrysanthemi* EC16 (formerly known as *Pectobacterium chrysanthemi* EC16 and *E. chrysanthemi* EC16) (Fig. 5) [26].

On the basis of the results of the siderophore activity evaluation of Vcb analogues, three conjugates **35**–**37** between the known antibiotic norfloxacin and Vcb analogues **23b** and **24b** were synthesized using acetate as a spacer arm. A four conjugate **38** was also prepared between norfloxacin and aminochelin (**39**), one of the siderophores produced by the Gram-negative free-living soil bacterium *Azotobacter vinelandii* [35]. Although aminochelin (**39**) displayed siderophore activity in *V. anguillarum* serotype O2, in contrast to the other Vcb two analogues, aminochelin does not use the OMR of Vcb (**2**) FvtA as the route of entry.

The coupling of 2,3-diisopropyloxybenzoic acid (**40**), obtained in a similar way as **9**, with *tert*-butyl(4-aminobutyl)carbamate gave carbamate **41**. The free amine obtained from the deprotection of the Boc group in **41** was coupled with chloroacetyl chloride and then with norfloxacin to give the aminochelin–norfloxacin conjugate **38** after the removal of isopropyl protecting groups with BCl_3. For the synthesis of DHBA-D-ornithine-norfloxacin conjugates **36** and **37**, N^{δ}-Cbz-D-ornithine-O^{t}Bu, prepared from the commercially available N^{δ}-Cbz-D-ornithine, was coupled with 2,3-diisopropyloxybenzoic acid (**40**) to give carbamate **42**. Removal of the Cbz group in **42** by catalytic hydrogenation gave a free amine which was submitted to the same procedure as before to afford an intermediate that yielded conjugates **36** and **37**, after removal of isopropyl protecting groups with BCl_3 in MeOH or H_2O,

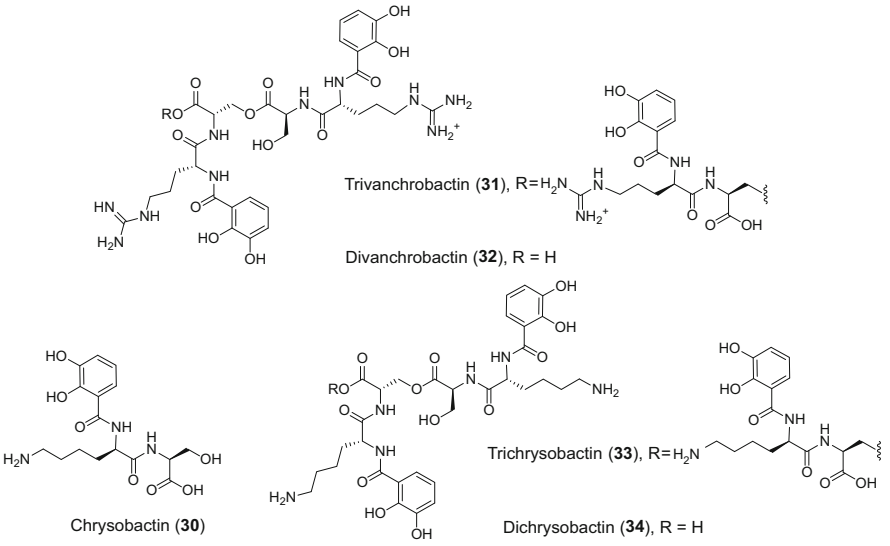

Fig. 5 Siderophores with similar structures to that of Vcb (**2**)

respectively. For the synthesis of DHBA-D-ornithine-norfloxacin conjugate **35**, N^{δ}-Cbz-D-ornithine-OMe (**16a**, Scheme 2) was coupled first with 2,3-diisopropyloxybenzoic acid (**40**) and then, after saponification, with O-*tert*-butyl-L-serine *tert*-butyl ester to give dipeptide **43**. Finally, the submission of the protected dipeptide **43** to the same sequence of reactions employed in the preparation of conjugate **38** from **41** gave conjugate **35** (Scheme 4). The four synthetic conjugates **35**–**38** gave a positive reaction in the CAS test indicating that the binding of the Vcb analogs to norfloxacin through the amino functionality did not affect the chelating ability of these compounds. However, the lower antibiotic activity displayed by the four conjugates **35**–**38** in relation to unconjugated norfloxacin indicates that they are not working as Trojan horse conjugates [36].

Vanchrobactin iron complexes studies using spectrophotometric and potentiometric methods were reported. Kinetic studies at different pHs showed that of free Vcb (**2**) is stable in the pH range from 4 to 10.4 while the presence of a single pK with a value of 6.79 was obtained by spectroscopic titration studies. The influence of pH on iron vanchrobactin complex formation, shown in its UV visible spectra, reflects the presence of three sequential complexation reactions, corresponding to the formation of the ferric mono-, bis-, and tris(Vcb) complexes. The color change from alkaline to acid media was a clear indication of a structural change under pH variation. The resulting potentiometric titration curve of ferric Vcb complexes indicates the stepwise formation of the ferric mono-, bis-, and tris(Vcb) complexes. A value of pFe(Vcb) of 20 (for enterobactin pFe for is 35.6) was obtained for Vcb (**2**) by modeling the Fe^{3+} uptake under physiological conditions [37].

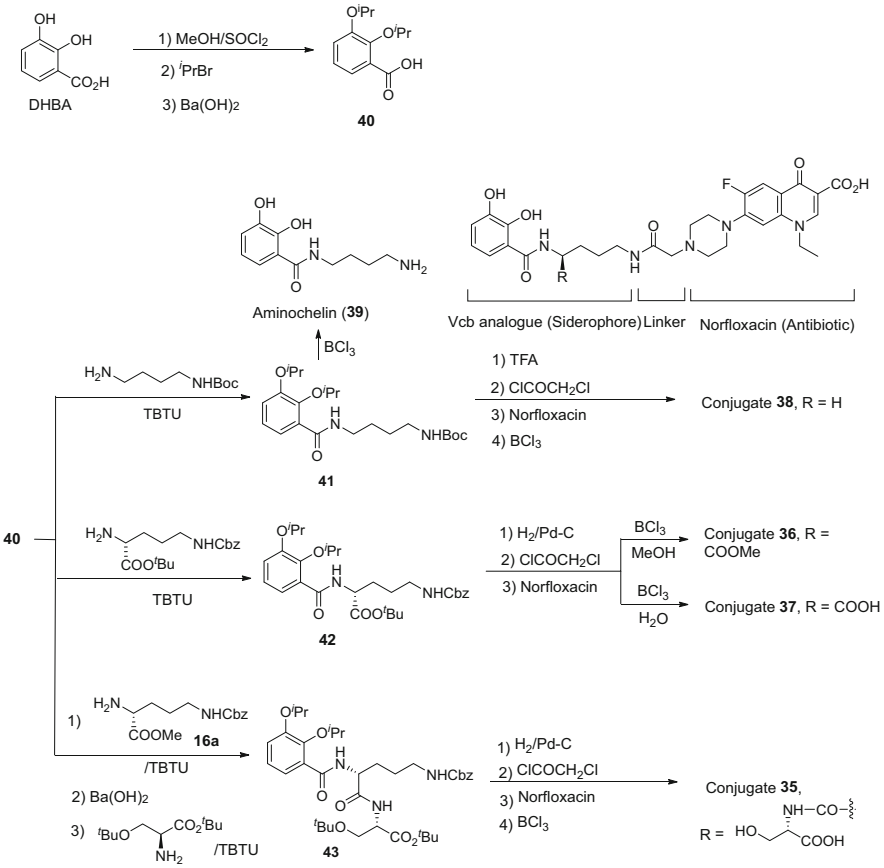

Scheme 4 Synthesis of the conjugates **35**–**38** between norfloxacin and Vcb analogues and aminochelin (**39**)

The biosynthesis and transport of Vcb (**2**) in strain RV22 is encoded by the *vab* gene cluster, a c. 26 kb chromosomal region, containing 13 genes. The *vabABCEF* genes are the main biosynthetic components which encode the enzymes necessary for DHBA biosynthesis and activation, and *vab*F, a gene encoding an NRPS involved in the assembly of the siderophore components [38]. The biosynthetic pathway proposal was very helpful in elucidating its structure. Indeed, the first proposed structure, 2,3-dihydroxybenzoyl- serinyl -arginine, was discarded for the corrected one, [(2,3-dihydroxybenzoyl)arginyl]serine, where the position of serine and arginine was interchanged because the domain responsible for incorporating the arginine residue is located first [29].

Vanchrobactin transport to the cell is achieved by means of the TonB-dependent outer membrane receptor (OMR) FvtA, a 78 kDa protein, encoded by the *fvt*A gene linked to the biosynthetic genes. The synthesis of Vcb (**2**) along with their analogues

described before and the preparation of a series of mutant strains were crucial in confirming the actual role of *fvt*A gene. The results indicated that FvtA seems to recognize primarily the catechol-iron center since it is not only the route of entry for Vcb (**2**) but also of the other Vb analogues [39].

2.3 Piscibactin Iron-Uptake System

When the complete genome sequence of the *V. anguillarum* RV22 strain was described [40], the in silico analysis of this genome showed that the second chromosome II contains an additional siderophore gene cluster that encodes Pcb (**3**), the siderophore responsible for the iron uptake of *Photobacterium damselae* subsp *piscicida* which will be discussed later in this chapter. The production of Pcb (**3**) in *V. anguillarum* RV22 wild type was demonstrated by chemical analysis using the SPE-HLB/HPLC-MS methodology of the cell-free supernatants of this bacterium, detecting its Ga (III) complex using the same methodology described in *P. damselae* subsp. *piscicida*. The analysis showed that both siderophores, Pcb (**3**) and Vcb (**2**), are produced simultaneously. In this way, it was demonstrated that Pcb (**3**) is actually the third siderophore produced by this *Vibrio* species [41].

2.4 Distribution of Each Siderophore Iron-Uptake System and Their Role in the Virulence

Although the ability of some pathogens to carry multiple iron acquisition systems seems redundant in laboratory culture conditions, the co-expression of siderophores with different chemical properties can play specialized roles at the host-pathogen interface. Indeed, the ability to produce more than one siderophore can enhance niche flexibility and pathogenesis of the bacteria.

The vanchrobactin biosynthesis and transport gene clusters (*vabB* and *fvtA*) are ubiquitous in both vanchrobactin- and anguibactin-producing *V. anguillarum* strains. However, anguibactin strains do not produce Vcb (**2**) because the *vab*F gene, which encodes the NRPS that assembles the siderophore molecule, is inactivated by the insertion of the transposable element encoded on the plasmid pJM1. On the other hand, piscibactin genes (*irp*-HPI) are not only widespread in *V. anguillarum* strains but also many other species of *Vibrio* [42]. Moreover, the piscibactin biosynthesis gene cluster is never present in anguibactin-producing strains. Most pathogenic *V. anguillarum* strains lacking the anguibactin system produce simultaneously both siderophores, Vcb (**2**) and Pcb (**3**).

It is assumed that the vanchrobactin mediated system is the ancestral iron-uptake mechanism mediated by siderophores of *V. anguillarum*. The anguibactin-mediated system could have been acquired later by *V. anguillarum*, likely by horizontal

transfer, during the evolution of this species, leading to the inactivation of the vanchrobactin system, since anguibactin-mediated iron transport seems to be more efficient due to the Ang (**1**) stronger affinity for iron. The Highly Pathogenically Island encoding piscibactin mediated system (*irp*-HPI) could also have been acquired by horizontal transfer [16].

On the other hand, *V. anguillarum* is able to modulate the synthesis of Vcb (**2**) and Pcb (**3**) according to the surrounding temperature. Expression of piscibactin biosynthetic genes is three times higher at 18 °C than at 25 °C. Thus, Pcb (**3**) is preferentially produced at low temperatures, which are the temperature that *V. anguillarum* finds during infection of fish cultivated cold-water temperatures. In contrast, when *V. anguillarum* grows at warm-water temperatures (approx. 25 °C), piscibactin genes are down-regulated (fourfold lower) in relation to Vcb (**2**) [41].

It has been demonstrated that the ability to produce Ang (**1**) is a prerequisite for the virulence of *V. anguillarum* serotype O1 plasmid bearing strains and so, Ang (**1**) is a key virulence factor for those strains. In relation to the efficiency or virulence of Vcb (**2**) versus Ang (**1**), it was found that when an anguibactin-producing *V. anguillarum* strain co-infects a fish with a vanchrobactin producing strain, the former is the only one recovered from diseased fish in the first days of infection [16].

On the other hand, Pcb (**3**) contributes to a greater extent than Vcb (**2**) to virulence in fish and also, the ability to produce Pcb (**3**) seems to be sufficient to confer maximum virulence to *V. anguillarum*. In fact, piscibactin genes are associated with a highly virulent phenotype for several fish species. Pcb (**3**) plays a relevant role in the cell fitness and contributes to a greater extent than Vcb (**2**) to the virulence for fish [41]. Experimental infections in turbot showed that although both siderophores are simultaneously produced, Pcb (**3**) is a key virulence factor to infect fish, while Vcb (**2**) seems to have a secondary role in virulence. A recent analysis of 44 *V. anguillarum* genomes confirmed this hypothesis [15]. Thus, it is likely that Vcb (**2**) biosynthesis could be more related to persistence in a marine environment than to pathogenesis [43].

3 Photobacteriosis by *Photobacterium damselae* subsp. *piscicida*

Photobacteriosis, formerly known as fish pasteurellosis, is a septicemia caused by the Gram-negative pathogenic halophilic bacterium *Photobacterium damselae* subsp. *piscicida* (Vibrionaceae). The disease was originally named after the classification of this aforesaid agent as *Pasteurella piscicida*. It acquired its present name following the reassignment to the genus *Photobacterium*. The presence of white nodules in the internal viscera, particularly, spleen and kidney in the fish is the reason why it is also known as pseudotuberculosis. Since 1969, photobacteriosis has been one of the most important diseases in Japan, affecting mainly to yellowtail (*Seriola quinqueradiata*), and from 1990 became the major pathological problem in

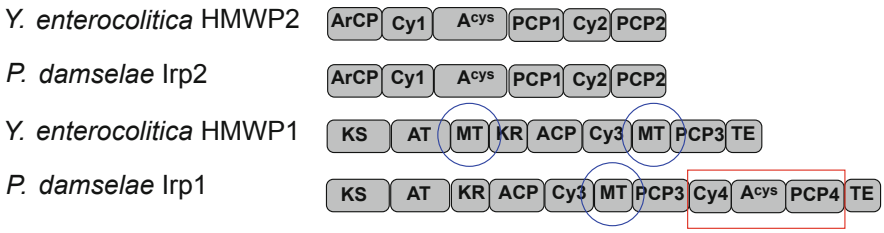

Fig. 6 Comparison of the domain composition of the multifunctional enzymes HMWP1 and HMWP2 of *Y. enterocolitica* and the corresponding Irp1 and Irp2 of strain DI21 of *P. damselae* subsp. *piscicida*

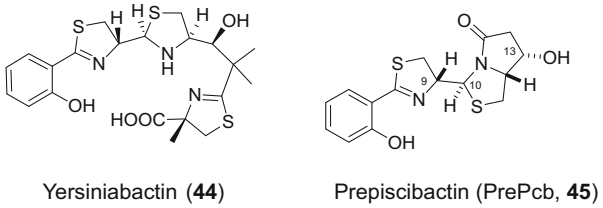

Fig. 7 Structures of yersiniabactin (**44**) and prepiscibactin (PrePcb, **45**)

the culture of gilthead sea bream (*Sparus aurata*), seabass (*Dicentrarchus labrax*), and sole (*Solea senegalensis* and *S. solea*) in the European Mediterranean countries, including Spain. Additionally, this pathogen is also able to infect a wide variety of marine fish such as striped bass (*Morone saxatilis*), white perch (*M. americana*), and hybrid striped bass (a hybrid between the striped bass (*M. saxatilis*) and the white bass (*M. chrysops*)) in the USA, cobia (*Rachycentron canadum*) in Taiwan, and golden pompano (*Trachinotus ovatus*) in China. Now, photobacteriosis is now considered one of the most dangerous bacterial diseases in aquaculture worldwide due to its wide host range, high mortality rate, and ubiquitous distribution [44].

The structure of the siderophore responsible for the iron uptake in *P. damselae* subsp. *piscicida*, named as piscibactin (**3**), was predicted from the study of genes in the strain DI21 involved in its biosynthesis which are organized in a typical structure of a Pathogenicity Island (PAI) [45]. Database searches revealed that this PAI shows a high degree of homology to the High Pathogenicity Island (HPI) described in *Yersinia* spp., such as *Yersinia pestis*, which encodes the synthesis of the siderophore yersiniabactin (**44**) [46]. More specifically, the structural prediction was deduced from the differences between the domain composition of the multifunctional enzymes HMWP1 and HMWP2 of *Y. enterocolitica* and the corresponding Irp1 and Irp2 of strain DI21 of *P. damselae* subsp. *piscicida*. Thus, the presence of just one methyltransferase domain (MT) in Irp1 of *P. damselae* subsp. *piscicida* DI21 strain instead of the two MT in HMWP1 of *Y. enterocolitica* (Fig. 6) suggested the lack of some methyl groups in the structure of Pcb (**3**) in relation to that of yersiniabactin (**44**) (Fig. 7). *Y. pestis* is the causative agent of the bubonic plague or Black Death that killed one third of the European population in the Middle Age,

while *Y. enterocolitica* causes severe enteric disorders in humans. Moreover, *P. damselae* subsp. *piscicida* can use yersiniabactin (**44**) as xenosiderophore [45].

Due to its high instability, Pcb (**3**) was isolated as its Ga^{3+} and Fe^{3+} complexes. Its Ga^{3+} complex made an NMR study possible, while a bioguided fractionation could be performed due to its Fe^{3+} complex. Thus, filtered supernatants of cell-free culture broth of *P. damselae* subsp. *piscicida* DI21 were incubated with the corresponding Ga^{3+} and Fe^{3+} salts and submitted to the SPE- HLB/HPLC-HRMS methodology where the use of acidic conditions being avoided at any time. Fractions containing the piscibactin Ga^{3+} complex were easily identified in the MS by the presence of the *m/z* cluster with the distinctive isotopic ratio of gallium (Mr = 69 and 71, ratio 3:2). The structure of Pcb (**3**) was established from the 1D/2D NMR and HR-ESIMS data analysis of its piscibactin-Ga(III) complex. Furthermore, a possible intermediate of its biosynthesis, called prepiscibactin (prePcb, **45**), was also isolated in the process (Fig. 7) [47].

The stereoselective synthesis of prePcb (**45**), whose structure is characterized by the presence of four stereogenic centers and three heterocycle rings, was reported. The chiral sources for positions (9*R*) and (12*R*) were L- and D-cysteines while the secondary alcohol at position (13*S*) was generated by a stereoselective SmI_2-mediated Reformatsky reaction. The synthesis of prePcb (**45**) started with the conversion of L-cysteine to acid **46** which was converted to the thiazolidinic aldehyde **47** through the Weinreb amide and posterior reduction. The crucial SmI_2-induced Reformatsky reaction between the thiazolidinic aldehyde **47** and (*R*)-chloroacetyl-2-oxazolidinone **48** resulted in the formation of the desired secondary alcohol **49** as a single diastereoisomer with a very high yield. Removal of the chiral auxiliary, the acetonide and Boc protecting groups afforded the thiol amino alcohol ethyl ester **50**. In parallel, condensation of D-cysteine and 2-hydroxy benzonitrile gave a thiazolinic carboxylic acid which was transformed to the thiazolidinic aldehyde **51** via the corresponding Weinreb amide followed by reduction. Finally, the coupling between the thiol amino **50** and the thiazolidinic aldehyde **51** in the presence of potassium acetate followed by refluxing in toluene gave prePcb (**45**) along with its epimer at C10 in a 1:1 ratio. The stereoselectivity of the required isomer prepiscibactin from 1:1 to 4:1 ratio was improved by addition of $ZnCl_2$ (Scheme 5) [48].

In the recently reported stereoselective convergent synthesis of Pcb (**3**), D-cysteine was used as a chiral source for the (9*R*) and (17*S*)-positions, L-cysteine was employed to generate the (12*R*)-position while Meldrum's acid was utilized in the preparation of the secondary alcohol at the (13*S*)-position. One of the major challenges of this synthesis was the presence of a high sensitive β-hydroxy-2,4-disubstituted thiazoline moiety in Pcb (**3**) lacking the bulky *gem*-dimethyl groups at C-14 present in yersiniabactin (**44**) [49].

The synthesis started with the protection of the thiol and the primary amine of L-cys with Trt and Fmoc protecting groups, respectively, to give Fmoc-Cys(Trt)-OH (**52**) which was subsequently coupled with Meldrum's acid to afford **53**. Refluxing **53** in EtOAc followed by stereoselective reduction of the resulting tetramic acid with $NaBH_4$ gave lactam **54** where the stereogenic centers present in Pcb (**3**) at C-12 and C-13 positions were efficiently generated. Then, the selective basic cleavage of the lactam **54** in the presence of the Fmoc group to afford statine **55** was performed by

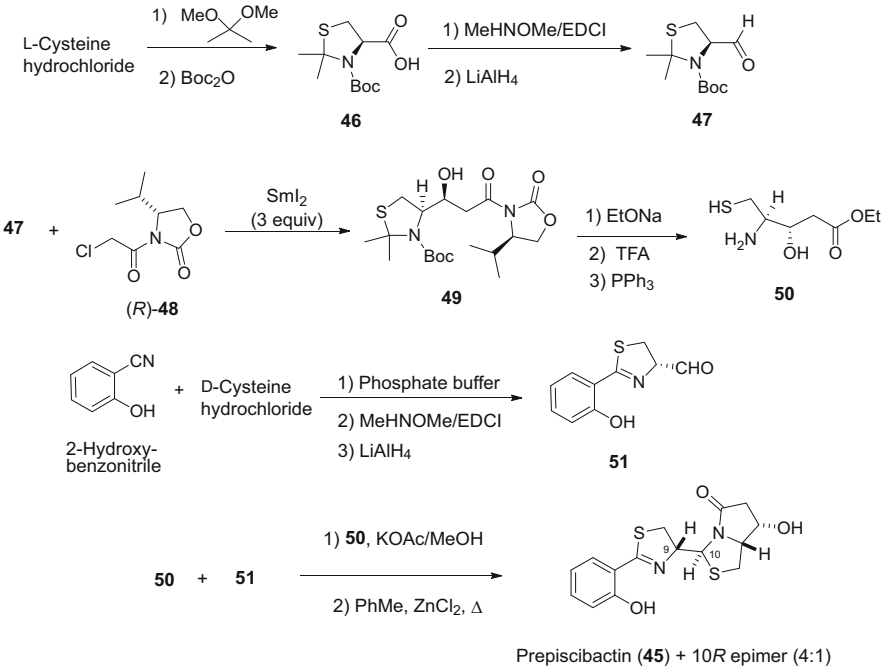

Scheme 5 Synthesis of PrePcb (**45**)

using LiOH with added $CaCl_2$. Posterior protection of the hydroxyl group as triethylsilyl (TES) ether in **55** yielded the conveniently protected carboxylic acid **56**. The next step implied the coupling of a freshly prepared solution of the methyl ester of (*S*)-α-azido-α-methylcysteine (**57**), obtained from D-cysteine following reported procedures, with statine **56**, previously activated with EDC, to furnish thioester **58**. The key step for the formation of the sensitive β-hydroxy-2,4-disubstituted thiazoline moiety implied the use of the mild and non-dehydrative conditions from the azide of thioester **58** via Staudinger reduction and the subsequent intramolecular aza-Wittig (S-AW process) with PPh_3 in 2,6-lutidine to give **59**. A very mild method for removal of protecting groups in **59** was carried out by deprotection of the Trt group using I_2 in CH_2Cl_2, followed by treatment of the resulting disulfide **60** with NaN_3 in the presence of the scavenger octanethiol and ending with deprotection of the TES ether with TBAF to give the methylester thiazoline **62**.

For the completion of the synthesis of **3**, thiazolinic aldehyde **51**, already described in the synthesis of prePcb (**45**), was coupled with methylester thiazoline **62**, both freshly prepared, to afford an epimeric mixture of methyl esters **63a,b** at C-9. Finally, basic hydrolysis of the ester mixture **63a,b** with LiOH gave the very unstable acid **3** and its C-9 epimer which were subjected without purification to complexation with gallium $Ga(acac)_3$. The resulting product was submitted to chromatographic separation using RP-C18 cartridges followed by HPLC

purification to deliver Pcb-Ga^{3+}-complex **64** which resulted to be identical to the natural product. In this way, the absolute configuration of Pcb (**3**) could be determined as (**9*R*,10*R*,12*R*,13*S*,17*S*)-3**. Additionally, when the product obtained from the basic hydrolysis with LiOH of methyl esters **63a,b** was subjected to complexation with gallium in CD_3OD furnished the deuterated Pcb-d_2 (**65**), where the two hydrogens at C-14 position were interchanged by two deuterium atoms. Pcb-d_2 (**65**) could be used as a new molecular tool to carry out further studies on the iron-uptake mechanisms.

Pcb (**3**) is a siderophore encoded by *irp* genes in a high-pathogenic island named *irp*-HPI [45] which is widespread among *Vibrionaceae* [42]. In *P. damselae* subsp. *piscicida*, the *irp*-HPI is part of a plasmid pPHDP70 [50]. It was suggested that this plasmid could be acquired by horizontal transfer, with an evolutionary origin similar to that of *Yersinia* HPI. The proposal of an assembly line for the biosynthesis of Pcb (**3**), showing the presence of just one methyltransferase (MT) domain in the multifunctional enzymes PKS/NRPS Irp1, agrees with the lack of the two methyl groups at C-14 in relation to that of yersiniabactin (**44**). Moreover, a cryptic metabolite was also predicted, although not detected yet, from the presence of additional module in Irp1 [47].

The plasmid pPHDP70 that encodes Pcb (**3**) biosynthesis could be transferred by conjugation from *P. damselae* subsp. *piscicida* to a mollusk pathogenic *Vibrio alginolyticus* mutant strain, where it was abolished the production of its native siderophore, vibrioferrin [51]. Acquisition of plasmid pPHDP70 by conjugation restored the capacity of that mutant to grow under low-iron conditions since it could synthesize Pcb (**3**). Piscibactin production was demonstrated by chemical analysis of its culture supernatants using the same SPE-HLB/HPLC-MS methodology employed in the isolation of gallium (III) and iron (III) piscibactin complexes from *P. damselae* subsp. *piscicida*. These experiments confirmed not only that the plasmid pPHDP70 is responsible for the production of Pcb (**3**) but also showed that the horizontal transfer of that plasmid by conjugation can be very easy and common [50].

Piscibactin production was proven as one of the major virulence factors not only in *V. anguillarum* but also in *Photobacterium damselae* subsp. *piscicida*. The key role of Pcb (**3**) in the virulence of this bacterium was demonstrated by the fact that *P. damselae* subsp. *piscicida* strains cured of pPHDP70 not only were incapable of producing Pcb (**3**) and growing under iron-limited conditions but also exhibited markedly decreased virulence in fish [50].

The plasmid pPHDP70 encodes a hitherto uncharacterized TonB-dependent transporter named FrpA that would act as the Pcb (**3**) outer membrane receptor (OMR) [45]. In order to find a new vaccine formulation as alternative to the existence one based on the use of inactivated bacterial cells, FrpA was cloned, expressed in *E. coli* using an arabinose-inducible promoter, and the resulting rFrpA purified from its cultures. Evaluation of its effectiveness against photobacteriosis and immunogenicity as vaccine on sole (*Solea senegalensis*) showed that the rFrpA protein is immunogenic, displaying an immunity response that was equivalent to that observed in fish immunized with the corresponding

bacterin, obtained from formalin-killed whole cells of *P. damselae* subsp. *piscicida*. Furthermore, experimental infection challenge trials showed that fish groups vaccinated with bacterin or rFrpA were protected against photobacteriosis with similar protection levels, reaching survival rates (RPS) of ca. 79% and 73%, respectively [52]. Indeed, rFrpA represents a promising antigen candidate for the development of novel more effective vaccines for the prevention of fish photobacteriosis. Although there are precedents for the use of OMR of siderophores from pathogenic bacteria as vaccines, this is one of the first applications against an infectious disease in fish [53].

4 Furunculosis by *Aeromonas salmonicida*

Furunculosis is a disease which causes economically devastating losses in cultivated salmonids in fresh and marine waters. It shows a widespread distribution. Although all salmonid species such as Atlantic salmon (*Salmo salar*), which is considered particularly susceptible, and rainbow trout (*Oncorhynchus mykiss*) can be affected, it also affects several non-salmonids species including turbot (*Scophthalmus maximus*) and halibut (*Hippoglossus hippoglossus*). The disease was first described by Lehmann and Neumann in 1896 and its name comes from the deep ulcerations that it causes on skin. Most Atlantic salmon infected by the disease presents a hemorrhagic septicemia with high mortality rates, in both juvenile and adult fish, within as little as 2 or 3 days [54].

The etiological agent of furunculosis is the non-motile rod Gram-negative γ-proteobacteria *Aeromonas salmonicida* subsp. *salmonicida* (*A. salmonicida*). This bacterium can be defined as biochemically, antigenically, and genetically homogeneous with no biotypes, serotypes, or genotypes. Three subspecies of *A. salmonicida*, *masoucida*, *achromogenes,* and *smithia*, named atypical strains, are also pathogenic [12].

The first studies of siderophore biosynthesis genes of *A. salmonicida* displayed the presence of a chromosomal gene cluster (*asb*GFDCBI) with high similarity to genes related to the synthesis of the siderophore Acb (**6**) from *A. baumannii* [55]. The completion of its genome sequence several years later revealed, by bioinformatic genomic analysis, the presence of a second gene cluster with high similarity to those of amonabactins (Fig. 8) from *Aeromonas hydrophila*. Finally, it was demonstrated that most *A. salmonicida* subsp. *salmonicida* strains produce two

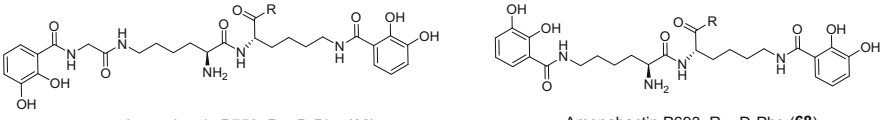

Amonabactin P750, R = D-Phe (**66**)
Amonabactin T789, R = D-Trp (**67**)

Amonabactin P693, R = D-Phe (**68**)
Amonabactin T732, R = D-Trp (**69**)

Fig. 8 Structure of the amonabactins biosynthetized (**66**–**69**) by *A. salmonicida* subsp. *salmonicida*

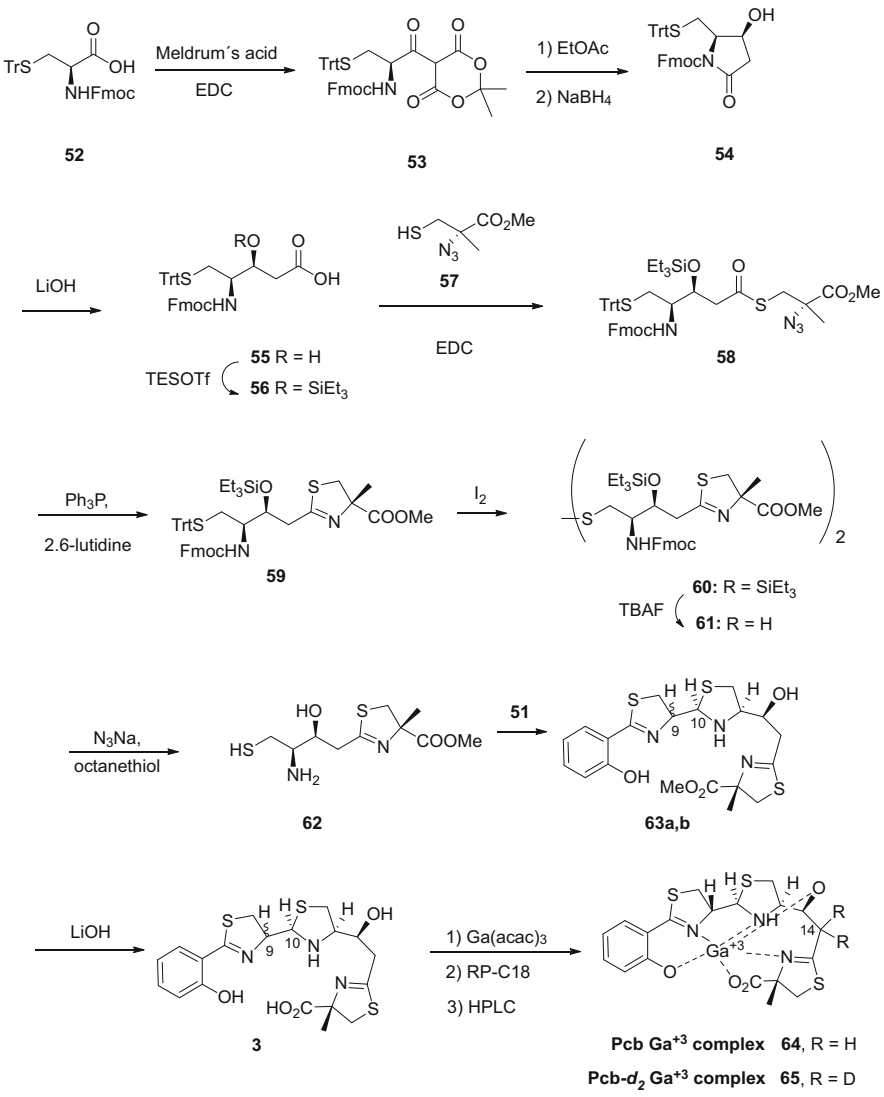

Scheme 6 Synthesis of Pcb (**3**) and its Ga^{+3} complex **64**

catechol siderophores simultaneously: Acb (**6**) and the four amonabactin variants that are denoted as P750, T789, P693, and T732 (**66**–**69**) according to the presence of either a Phe or Trp residue and their molecular weights (by the presence or absence of a Gly residue) [56].

The initial structure assigned for Acb as **5** when it was first described in 1994 from the human pathogen *A. baumannii* ATCC19606 [57] was corrected in 2009 as **6**. It was suggested that **5**, named as now preacinetobactin (preAcb, **5**), is an unstable

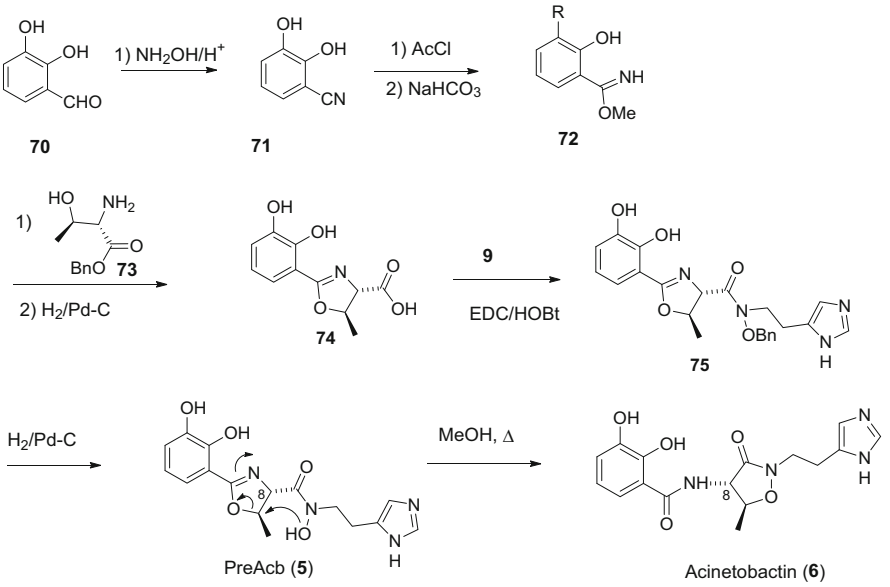

Scheme 7 Synthesis of Acb (**6**)

oxazoline which suffers an intramolecular nucleophilic substitution to give isoxazolidinone Acb (**6**) (see Scheme 7) [58]. A complete study of the Acb (**6**) isomerization at different pH was published in 2015 [59]. On the other hand, the four amonabactins (**52**–**55**) were previously isolated and characterized from the pathogenic bacterium of animals and humans *A. hydrophila* by Raymond and coworkers in 1994 [60].

Acb (**6**) was isolated from the virulent strain *A. salmonicida* RSP74.1 which does not produce amonabactins due to a natural deletion in the *amoG* gene. The amonabactins were isolated and/or detected from the mutant strain *A. salmonicida* VT45.1ΔasbD. This mutant was obtained from another highly virulent strain, *A. salmonicida* VT45.1, which produces simultaneously both siderophores, where it was abolished the Acb biosynthesis (deletion of the *asbD* gene) to facilitate the isolation of the amonabactins. The methodology SPE-HLB/HPLC-HRMS [30] was successfully applied in both cases confirming its high efficiency to accelerate the isolation process of siderophores containing catecholate/salicylate moieties [56].

The structure of Acb as **6**, including its absolute configuration, was confirmed by chemical synthesis developed by Takeuchi et al. [24]. This synthesis started from 2,3-dihydroxybenzaldehyde (**70**) which was transformed to the imidate **72** via the nitrile **71**. Condensation of L-threonine benzyl ester (**73**) with imidate **72** gave an oxazoline intermediate which was submitted to hydrogenolysis to afford the oxazoline acid **74**. Then, imidazole **9**, whose preparation was described in the synthesis of Ang (**1**) displayed in Scheme 1, was coupled with acid **74** to yield the

oxazoline protected **75**. Finally, benzoyl deprotection by hydrogenolysis of **75** gave preAcb (**5**) which under reflux in MeOH afforded Acb (**6**) (Scheme 7).

Although the synthesis of the four natural amonabactins were first reported by Telford and Raymond in 1997 [61], an improved variation of that synthesis was published in 2019 [62]. The more recent synthesis of amonabactins started with the preparation of the activated building blocks **77** and **79**. Thus, activation with *N*-hydroxysuccinimide (NHS) of the isopropyl-protected 2,3-dihydroxybenzoic acid **40** (see Scheme 4) affording **76** and posterior coupling with commercially available N^{α}-Boc-L-lysine gave, after activation of the carboxylic acid with NHS, the first building block **77**. In parallel, activation of the carboxylic acid of commercially available N^{α}-Cbz-glycine with NHS and posterior coupling with N^{α}-Boc-L-lysine afforded, after hydrogenolysis of the Cbz group, the protected dipeptide **78**. This dipeptide was coupled with the NHS activated isopropyl-protected 2,3-dihydroxybenzoic acid **76** followed by activation with NHS to give the second building block **79**. Condensation of D-phenylalanine *tert*-butyl ester with the first building block **77** gave, after selective removal of the Boc protecting group, the protected dipeptide **80**. Coupling of dipeptide **80** with building blocks **79** or **77** yielded amonabactins P750 (**66**) and P6903 (**68**) (bearing a Phe residue), respectively, after the simultaneous removal of the isopropyl and *tert*-butyl protecting groups with BCl_3. In a similar way, the commercially available D-tryptophan methyl ester was coupled with the first building block **77** to give, after Boc deprotection, the dipeptide **81**. Dipeptide **81** was coupled with building blocks **79** or **77** to afford amonabactins T789 (**67**) and T732 (**69**) (bearing a Tyr residue), respectively, after basic hydrolysis of methyl ester with LiOH and removal of the isopropyl protecting groups with BCl_3 (Scheme 8).

The biosynthesis of both types of siderophores in *A. salmonicida* depends on *entABCE* genes, located within the amonabactin gene cluster, which encode the functions necessary for the synthesis of 2,3-dihydroxybenzoic acid (DHBA). Once DHBA is synthesized, *asbBCD* and *amoFGH* genes encode acinetobactin and amonabactins synthesis, respectively. Indeed, both siderophores share the first step of their biosynthesis, with the production of DHBA being the amonabactin gene cluster that supplies DHBA for both siderophores. Although both, acinetobactin and amonabactin, siderophore systems are present in all *A. salmonicida* strains, some isolates carry a mutation in the *amoG* gene that inactivates amonabactin synthesis. Interestingly, all *A. salmonicida* strains analyzed up to this point are able to use amonabactin as an iron source. The amonabactin biosynthesis genes are highly conserved in most *Aeromonas* species including the human pathogen *A. hydrophila*. On the contrary, Acb (**6**) is encoded by a gene cluster restricted to *A. salmonicida.* From the analysis of the genomic context of acinetobactin cluster, it seems clear that this gene cluster was likely acquired from other bacteria through horizontal gene transfer at some point during the speciation process of *A. salmonicida* while amonabactin must be the ancestral siderophore of the species [56].

Although FstB and FstC were previously identified as two outer membrane proteins specifically induced under iron deficiency and under in vivo conditions,

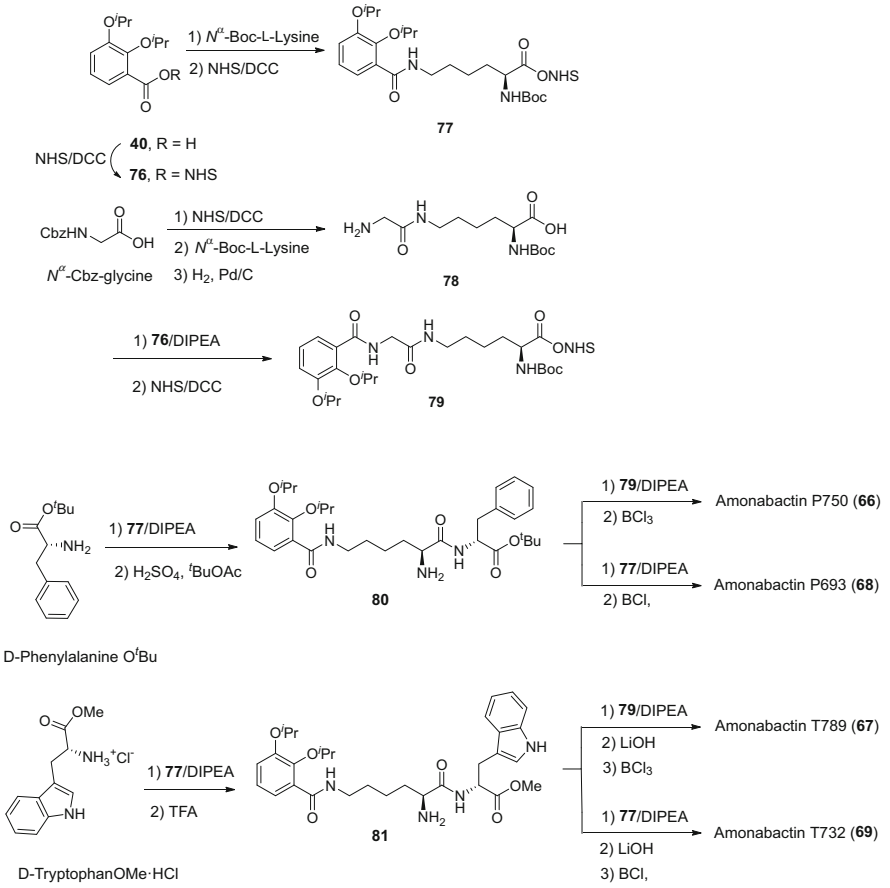

Scheme 8 Synthesis of amonabactins (**66–69**)

their role in the internalization mechanisms of ferric-acinetobactin and ferric-amonabactin was recently demonstrated. The TonB-dependent outer membrane receptor (OMR) protein FstB was identified and characterized as the receptor protein of Acb (**6**) in *A. salmonicida*. Even though this protein was initially named FstA, FstA and FstB are probably two versions or alleles of the same protein [63]. On the other hand, FstC is the OMR of all four amonabactin forms. The FstC receptor is widespread in the genus *Aeromonas*, not only among *A. salmonicida* strains but also in most *Aeromonas* species, including relevant human and animal pathogens as *A. hydrophila* [62].

Several analogues of Acb (**6**) and amonabactins (**66–69**) were prepared based on their simplicity in order to deduce some correlations between the structure and the siderophore activity to facilitate the preparation of conjugates for the development of novel applications of the bacterial iron-uptake mechanisms based on siderophores.

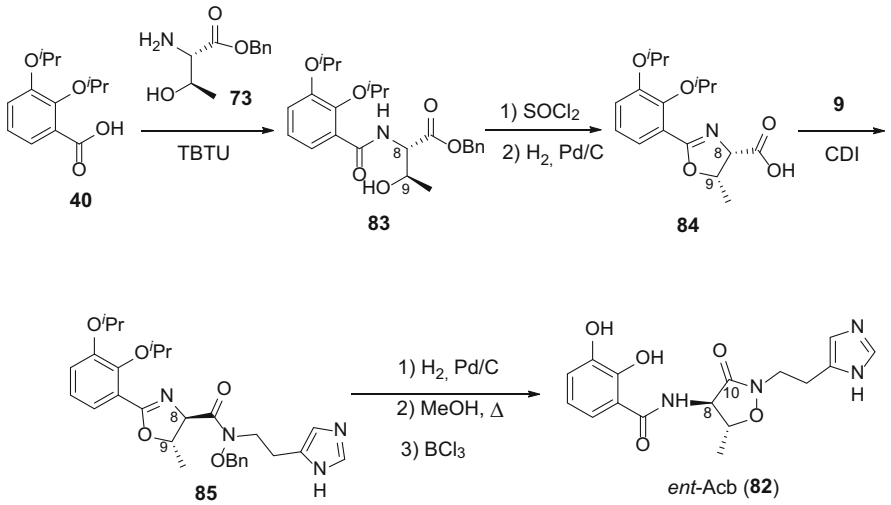

Scheme 9 Synthesis of *ent*-Acb (**68**)

In order to evaluate the influence of the stereogenic centers on the siderophore activity of Acb (**6**), its enantiomer, *ent*-Acb (**82**), was synthetized using a similar strategy employed in the synthesis of Acb (**6**) and Ang (**1**). Condensation of 2,3-diisopropyloxybenzoic acid (**40**) with L-threonine benzyl ester (**73**) gave amide **83** which was submitted to dehydrative-cyclization followed by debenzylation by hydrogenolysis to afford the oxazoline acid **84**. An inversion of configuration of the oxymethine carbon at C-9 took place in **84** during the cyclization process. Coupling of N^{α}-benzyloxyhistamine (**9**) (Scheme 1) with oxazoline acid **84** using CDI in the absence of base gave the sterically stable *trans*-isomer **85** rather than the *cis*-isomer, probably due to epimerization of the activated acyl intermediate. Debenzylation of oxazoline **85** by hydrogenolysis followed by reflux in MeOH gave the expected rearrangement of oxazoline to isoxazolidinone which was treated with BCl_3 to remove the isopropyl groups to yield *ent*-Acb (**82**) (Scheme 9).

With the aim of comparing the influence of the methyl group on the isoxazolidinone ring and the presence of similar heterocyclic rings, such as triazol instead of imidazole, on the siderophore activity of Acb analogues, four demethylacinetobactin derivatives (compounds **86**–**89**) were prepared. They were synthetized from a common intermediate **90** which was prepared by coupling of 2,3-dibenzyloxybenzoic acid (**17**) (Scheme 2) and the commercially available D-cycloserine. *N*-alkylation of intermediate **90** with mesylate **91**, prepared by mesylation of the commercial 3-benzyloxycarbonylaminopropanol, followed by subsequent removal of Cbz and Bn protecting groups by hydrogenolysis, gave the first demethylacinetobactin **86**. The second demethylacinetobactin **87** was synthetized by *N*-alkylation of intermediate **90** with the substituted imidazole

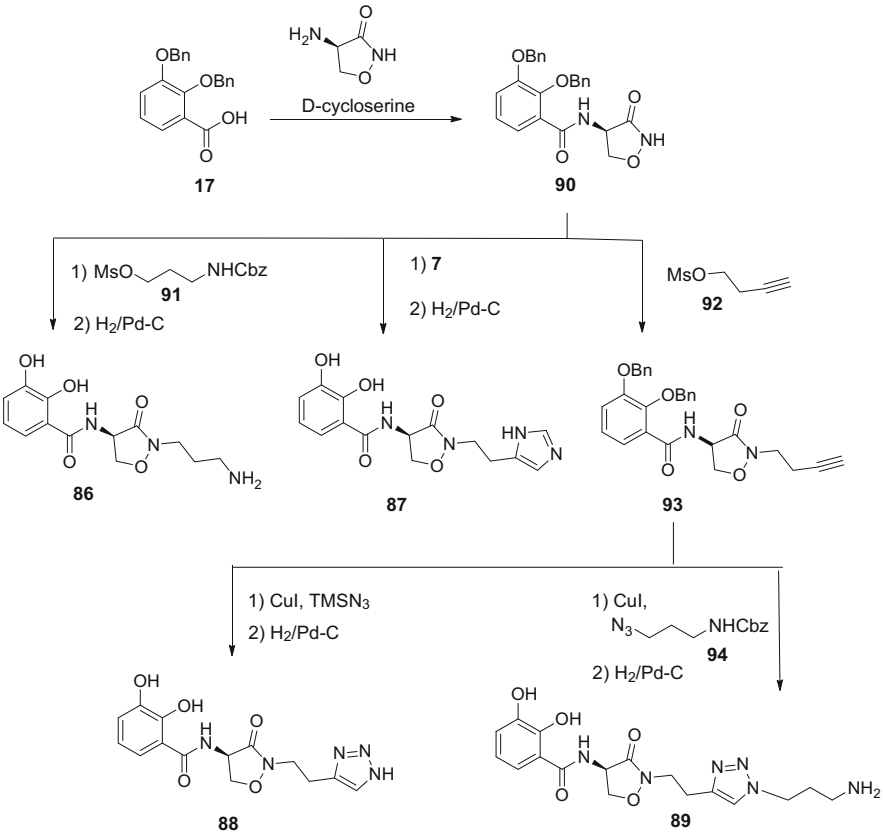

Scheme 10 Synthesis of demethylacinetobactin derivatives **86–89**

7 (see Scheme 1) and posterior debenzylation by hydrogenolysis. Demethylacinetobactin derivatives **88** and **89** were synthetized by using the "click-chemistry" reaction involving the efficient Cu(I)-catalyzed azide-alkyne couplings. Thus, *N*-alkylation of **90** with the mesylate **92**, obtained by mesylation of the commercial homopropargyl alcohol, gave the alkyne **93**. Coupling of trimethysilyl azide or azide derivative **94**, prepared by displacement of the mesylate group in **91** with sodium azide, with alkyne **93** afforded demethylacinetobactin analogues **88** and **89**, respectively, after removal of the protecting groups by hydrogenolysis (Scheme 10).

Several structure-activity relationships in relation to the OMR protein FstB implied in the internalization of ferric-Acb were deduced from the evaluation of the biological activity of synthetic *ent*-Acb (**82**) and four demethylacinetobactin analogues (**86–89**). All of them showed CAS values indistinguishable from those of Acb (**6**), indicating that they bind iron efficiently. The *ent*-Acb (**82**) displayed the same siderophore activity as the natural one, suggesting the lack of enantiomer

preference on the molecular recognition by the protein receptor FstB. The recognition of Acb (**6**) by its cognate OMR protein FstB mostly resides in the presence of imidazole (**87**) or a similar heterocyclic ring (**88**) in its structure because the presence of a primary amino group (**86**) or a propylamino substituted triazole (**89**) was devoid of such activity. Moreover, removal of the methyl group at the isoxazolidinone, in combination with the presence of either an imidazole or a triazole ring (**87** and **88**), leads to higher levels of biological activity. Additionally, it was suggested an alternative route(s) of entry for analogues **87** and **88** since they displayed siderophore activity in the growth promotion assay of a mutant strain which is unable to produce or transport acinetobactin [63].

On the other hand, with the aim of evaluating the minimum structural requirements for amonabactin recognition by its OMR protein FstC, four simplified analogues of the amonabactins were synthetized, compounds **95–99** using a similar synthetic sequence as that described for the natural ones.

Coupling the activated NHS carboxylic acid intermediate **76** with the commercially available *N*-Boc cadaverine (**99**) gave amide **100** which was treated with BCl_3 for removal of isopropyl and Boc protecting groups to give monocatecholate amonabactin analogue **95**. Removal of the Boc protecting group in **100** with TFA gave an intermediate which was coupled with activated NHS carboxylic acid intermediates **77** or **79** (Scheme 8) to give biscatecholate amonabactin analogues **97** and **98**, respectively, after deprotection with BCl_3. Finally, activation of N^{α}-Cbz-glycine with NHS, posterior coupling with *N*-Boc cadaverine (**99**) followed by deprotection of the Cbz group by hydrogenolysis gave amide **101** which was coupled with activated NHS carboxylic acid **76** to yield monocatecholate amonabactin analogue **96** after treatment with BCl_3 (Scheme 11).

Important structure-activity correlations were deduced from the evaluation of the biological activity of each of the four natural amonabactins individually **66–69** and of the four synthetic amonabactin analogues **95–99**. The lack of siderophore activity for monocatecholate amonabactin analogues **95** and **96** indicated that the presence of at least two catechol moieties is necessary to display biological activity. A quite different growth promotion activity was observed for each natural amonabactin form. The results suggested that natural amonabactins in which the length of the linker between the two iron-binding catecholamide units is 15 atoms, P750 (**66**) and T789 (**67**), instead of 12 atoms, P693 (**68**) and T732 (**69**), recognize more efficiently the OMR protein FstC. This was confirmed from the results obtained from the siderophore activity evaluation of the synthetic amonabactin analogues **97** and **98**. Indeed, the higher biological activity displayed by the bis-catechol amonabactin analogue **98** with longer linker (15 atoms linker length) in relation to that of bis-catechol amonabactin analogue **97** with a shorter linker (12 atoms linker length) is in agreement with the hypothesis that the length of the linker backbone (presence or absence of glycine) between the two iron-binding catecholamide units is relevant to maximize ferric-siderophore acquisition. Even though the presence of Phe or Trp residues seems not be required for siderophore recognition, their presence could also participate in the recognition by the receptor since biscatecholate amonabactin analogues **97** and **98** show less biological activity than their natural counterparts.

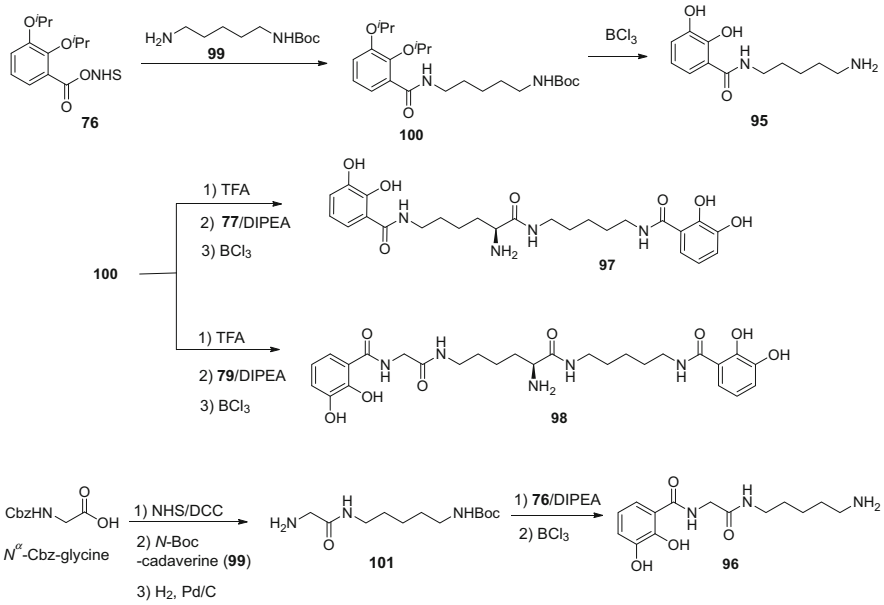

Scheme 11 Synthesis of amonabactin analogues **95**–**98**

In summary, three important conclusions were deduced from these studies. Firstly, the OMR protein FstC possesses a considerable functional plasticity that could be exploited for delivery of antimicrobial compounds into the cell. Second, the optimum linker length between the two catecholamide units for maximizing the siderophore activity in the amonabactin type-structures is 15 atoms, preferentially a Lys-Lys-Gly fragment which is present in the natural longer amonabactins **66** and **67** and analogue **98**. Finally, the synthetic simplified analogues **97** and **98** could be used as vectors for the preparation of conjugates in the Trojan horse strategy to develop new effective antimicrobials against many different pathogens of the genus *Aeromonas* including the human pathogen *A. hydrophila,* and for the synthesis of fluorescence probes to study the iron-uptake mechanism in this bacterium [62].

5 Concluding Remarks

The iron-uptake pathway is a key process for microbial survival and virulence. The knowledge of the mechanisms of iron acquisition mediated by siderophores can be of great help for the design of new strategies against microbial infections.

Fish disease outbreaks, vibriosis, photobacteriosis, and furunculosis, are considered as the major threats alarming the aquaculture industry and food security. Chemical and biological studies of the Gram-negative bacteria responsible for

Table 1 Siderophores from pathogenic bacteria involved in the main aquaculture infectious fish disease

Bacterium (fish disease)	Siderophore	OMR proteins	Biosynthetic gene cluster	Synthesis (Ref.)	Synthesis of analogues (Ref.)
V. anguillarum (vibriosis)	Anguibactin (**1**)	FatA	*AngBDEMNR* in the pJM1 plasmid	[25]	
	Vanchobactin (**2**)	FtvA	*VabABCEF* in the chromosome	[31]	[32]
	Piscibactin (**3**)			[49]	[48]
P. damselae subsp. *piscicida* (photobacteriosis)	Piscibactin (**3**)	FrpA	*Irp*-HPI in the pPHDP70 plasmid	[49]	[48]
A. salmonicida (furunculosis)	Acinetobactin (**6**)	FstB	*EntABCE asbBCD*	[24]	[63, 64]
	Amonabactins (**66–69**)	FstC	*EntABCE amoFGH*	[61, 62]	[62]

these infectious diseases allowed not only the isolation, structural elucidation and synthesis of the siderophores involved in their iron-siderophore uptake mechanisms but also the identification of their corresponding OMR proteins and the gene cluster involved in their biosynthesis (Table 1). All this information is being used in the development of new antimicrobial and vaccines based on the iron-siderophore uptake mechanism of these bacteria.

It is worth mentioning the great structural similarity of the siderophores biosynthesized by both human and fish virulent pathogenic bacteria. The structure of yersiniabactin (**44**), the siderophore produced by *Yersinia pestis*, responsible for epidemics of high mortality throughout the history of mankind (the plague of Justinian, the Black Death and the third pandemic), is very similar to that of Pcb (**3**) whose production confers maximum virulence in both *V. anguillarum* and *P. damselae* subsp. *piscicida*. Moreover, pyochelin, one of the siderophores produced by the human multidrug resistant bacteria pathogen *Pseudomonas aeruginosa*, is also structurally related to Pcb (**3**). One of the siderophores produced by *A. salmonicida*, Acb (**2**), is also biosynthesized by the human pathogen *A. baumannii*. This bacterium has been identified as one of the group of pathogens with a high rate of resistance to antibiotics and responsible for the majority of nosocomial infections. Moreover, the structure of Acb (**2**) is closely related to that of Ang (**1**) produced by some virulent strains of *V. anguillarum*. The fact that the anguibactin and piscibactin iron-uptake systems in *V. anguillarum* and the acinetobactin iron-uptake system to *A. salmonicida* had been probably acquired by horizontal transfer from other pathogenic bacteria seems to confirm the high efficiency of these iron absorption pathways.

Acknowledgements This work was supported by grants RTI2018-093634-B-C22 (AEI/FEDER, EU) from the State Agency for Research (AEI) of Spain, co-funded by the FEDER Programme from the European Union.

References

1. FAO. The State of World Fisheries and Aquaculture [Internet]. 2020 [cited 17 Oct 2020]. http://www.fao.org/state-of-fisheries-aquaculture/es/
2. Santos L, Ramos F (2018) Antimicrobial resistance in aquaculture: current knowledge and alternatives to tackle the problem. Int J Antimicrob Agents 52(2):135–143
3. Watts JEM, Schreier HJ, Lanska L, Hale MS (2017) The rising tide of antimicrobial resistance in aquaculture: sources, sinks and solutions. Mar Drugs 15(6):158
4. Wilson BR, Bogdan AR, Miyazawa M, Hashimoto K, Tsuji Y (2016) Siderophores in Iron metabolism: from mechanism to therapy potential. Trends Mol Med 22(12):1077–1090
5. Hider RC, Kong X (2010) Chemistry and biology of siderophores. Nat Prod Rep 27(5):637–657
6. Ji C, Juárez-Hernández RE, Miller MJ (2012) Exploiting bacterial iron acquisition: siderophore conjugates. Future Med Chem 4(3):297–313
7. Sandy M, Butler A (2009) Microbial iron acquisition: marine and terrestrial siderophores. Chem Rev 109(10):4580–4595
8. Bentur Y, McGuigan M, Koren G (1991) Deferoxamine (Desferrioxamine). Drug Saf 6 (1):37–46
9. Schalk IJ (2018) Siderophore–antibiotic conjugates: exploiting iron uptake to deliver drugs into bacteria. Clin Microbiol Infect 24(8):801–802
10. Cefiderocol Approval Letter (2020) [Internet]. https://www.accessdata.fda.gov/drugsatfda_docs/nda/2019/209445Orig1s000ltr.pdf. Accessed 17 Oct 2020
11. Fetcroja (cefiderocol) (2020) European Union [Internet]. https://www.ema.europa.eu/en/medicines/human/EPAR/fetcroja. Accessed 17 Oct 2020
12. Toranzo AE, Magariños B, Romalde JL (2005) A review of the main bacterial fish diseases in mariculture systems. Aquaculture 246(1–4):37–61
13. Mohamad N, Amal MNA, Yasin ISM, Zamri Saad M, Nasruddin NS, Al-saari N et al (2019) Vibriosis in cultured marine fishes: a review. Aquaculture 512:734289
14. Hickey ME, Lee JL (2018) A comprehensive review of *Vibrio* (*Listonella*) *anguillarum*: ecology, pathology and prevention. Rev Aquac 10(3):585–610
15. Hansen MJ, Kudirkiene E, Dalsgaard I (2020) Analysis of 44 *Vibrio anguillarum* genomes reveals high genetic diversity. PeerJ 8:e10451
16. Lemos ML, Balado M, Osorio CR (2010) Anguibactin- versus vanchrobactin-mediated iron uptake in *Vibrio anguillarum*: evolution and ecology of a fish pathogen. Environ Microbiol Rep 2(1):19–26
17. Actis LA, Fish W, Crosa JH, Kellerman K, Ellenberger SR, Hauser FM, Sanders-Loehr J (1986) Characterization of anguibactin, a novel siderophore from *Vibrio anguillarum* 775(pJM1). J Bacteriol 167(1):57–65
18. Jalal MAF, Hossain MB, Van der Helm D, Sanders-Loehr J, Actis LA, Crosas JH (1989) Structure of anguibactin, a unique plasmid-related bacterial siderophore from the fish pathogen *Vibrio anguillarum*. J Am Chem Soc 111(2):292–296
19. Hossain MB, Jalal MAF, Van Der Helm D (1998) Gallium-complex of anguibactin, a siderophore from fish pathogen *Vibrio anguillarum*. J Chem Crystallogr 28(1):57–60
20. Shrivastava SR, Shrivastava PS, Ramasamy J (2018) World Health Organization releases global priority list of antibiotic-resistant bacteria to guide research, discovery, and development of new antibiotics. J Med Soc 32:76–77

21. Noël S, Guillon L, Schalk IJ, Mislin GLA (2011) Synthesis of fluorescent probes based on the pyochelin siderophore scaffold. Org Lett 13(5):844–847
22. Lamb AL (2015) Breaking a pathogen's iron will: inhibiting siderophore production as an antimicrobial strategy. Biochim Biophys Acta 1854(8):1054–1070
23. Sassone-Corsi M, Chairatana P, Zheng T, Perez-Lopez A, Edwards RA, George MD, Nolan EM, Raffatellu M (2016) Siderophore-based immunization strategy to inhibit growth of enteric pathogens. Proc Natl Acad Sci 113(47):13462–13467. https://doi.org/10.1073/pnas.1606290113
24. Takeuchi Y, Ozaki S, Satoh M, Mimura K, Hara S, Abe H, Nishioka H, Harayama T (2010) Synthesis of acinetobactin. Chem Pharm Bull (Tokyo) 58(11):1552–1553
25. Lee H, Song WY, Kim M, Lee MW, Kim S, Park YS, Kwak K, Oh MH, Kim HJ (2018) Synthesis and characterization of anguibactin to reveal its competence to function as a thermally stable surrogate Siderophore for a gram-negative pathogen, *Acinetobacter baumannii*. Org Lett 20(20):6476–6479
26. Sandy M, Butler A (2011) Chrysobactin siderophores produced by *Dickeya chrysanthemi* ec16. J Nat Prod 74(5):1207–1212
27. Crosa JH. Deferration using anguibactin siderophore US5393777 A 1995-02-28; United States
28. Stork M, Di Lorenzo M, Welch TJ, Crosa LM, Crosa JH (2002) Plasmid-mediated iron uptake and virulence in *Vibrio anguillarum*. Plasmid 48(3):222–228
29. Soengas RG, Anta C, Espada A, Paz V, Ares IR, Balado M, Rodríguez J, Lemos ML, Jiménez C (2006) Structural characterization of vanchrobactin, a new catechol siderophore produced by the fish pathogen *Vibrio anguillarum* serotype O2. Tetrahedron Lett 47(39):7113–7116
30. Espada A, Anta C, Bragado A, Rodríguez J, Jiménez C (2011) An approach to speed up the isolation of hydrophilic metabolites from natural sources at semipreparative level by using a hydrophilic-lipophilic balance/mixed-mode strong cation exchange-high-performance liquid chromatography/mass spectrometry system. J Chromatogr A 1218(13):1790–1794
31. Soengas RG, Anta C, Espada A, Nieto RM, Larrosa M, Rodríguez J, Jiménez C (2007) Vanchrobactin: absolute configuration and total synthesis. Tetrahedron Lett 48(17):3021–3024
32. Soengas RG, Larrosa M, Balado M, Rodriguez J, Lemos ML, Jimenez C (2008) Synthesis and biological activity of analogues of vanchrobactin, a siderophore from *Vibrio anguillarum* serotype O2. Org Biomol Chem 6(7):1278–1287
33. Persmark M, Expert D, Neilands JB (1989) Isolation, characterization, and synthesis of chrysobactin, a compound with siderophore activity from *Erwinia chrysanthemi*. J Biol Chem 264(6):3187–3193
34. Sandy M, Han A, Blunt J, Munro M, Haygood M, Butler A (2010) Vanchrobactin and anguibactin siderophores produced by *Vibrio* sp. DS40M4. J Nat Prod 73(6):1038–1043
35. Page WJ, Tigerstrom MV (1988) Aminochelin, a catecholamine Siderophore produced by *Azotobacter vinelandii*. Microbiology 134(2):453–460
36. Souto A, Montaos MA, Balado M, Osorio CR, Rodríguez J, Lemos ML, Jiménez C (2013) Synthesis and antibacterial activity of conjugates between norfloxacin and analogues of the siderophore vanchrobactin. Bioorg Med Chem 21(1):295–302
37. Iglesias E, Brandariz I, Jiménez C, Soengas RG (2011) Iron(iii) complexation by Vanchrobactin, a siderophore of the bacterial fish pathogen *Vibrio anguillarum*. Metallomics 3(5):521–528
38. Balado M, Osorio CR, Lemos ML (2006) A gene cluster involved in the biosynthesis of vanchrobactin, a chromosome-encoded siderophore produced by *Vibrio anguillarum*. Microbiology 152(12):3517–3528
39. Balado M, Osorio CR, Lemos ML (2009) FvtA is the receptor for the siderophore vanchrobactin in *Vibrio anguillarum*: utility as a route of entry for vanchrobactin analogues. Appl Environ Microbiol 75(9):2775–2783
40. Naka H, Dias GM, Thompson CC, Dubay C, Thompson FL, Crosa JH (2011) Complete genome sequence of the marine fish pathogen *Vibrio anguillarum* harboring the pJM1 virulence

plasmid and genomic comparison with other virulent strains of *V. anguillarum* and *V. ordalii*. Infect Immun 79(7):2889–2900
41. Balado M, Lages MA, Fuentes-Monteverde JC, Martínez-Matamoros D, Rodríguez J, Jiménez C, Lemos ML (2018) The siderophore piscibactin is a relevant virulence factor for *Vibrio anguillarum* favored at low temperatures. Front Microbiol 9:1766
42. Thode SK, Rojek E, Kozlowski M, Ahmad R, Haugen P (2018) Distribution of siderophore gene systems on a Vibrionaceae phylogeny: database searches, phylogenetic analyses and evolutionary perspectives. PLoS One 13(2):e0191860
43. Ruiz P, Balado M, Fuentes-Monteverde JC, Toranzo AE, Rodríguez J, Jiménez C, Avendaño-Herrera R, Lemos ML (2019) The fish pathogen *Vibrio ordalii* under iron deprivation produces the siderophore piscibactin. Microorganisms 7(9):313
44. Andreoni F, Magnani M (2014) Photobacteriosis: prevention and diagnosis. J Immunol Res 793817
45. Osorio CR, Juiz-Río S, Lemos ML (2006) A siderophore biosynthesis gene cluster from the fish pathogen *Photobacterium damselae* subsp. *piscicida* is structurally and functionally related to the *Yersinia* high-pathogenicity island. Microbiology 152(11):3327–3341
46. Miller DA, Walsh CT, Luo L (2001) C-methyltransferase and cyclization domain activity at the intraprotein PK/NRP switch point of yersiniabactin synthetase [2]. J Am Chem Soc 123 (34):8434–8435
47. Souto A, Montaos MA, Rivas AJ, Balado M, Osorio CR, Rodríguez J, Lemos ML, Jiménez C (2012) Structure and biosynthetic assembly of piscibactin, a siderophore from *Photobacterium damselae* subsp. *piscicida*, predicted from genome analysis. Eur J Org Chem:5693–5700
48. Segade Y, Montaos MA, Rodríguez J, Jiménez C (2014) A short stereoselective synthesis of prepiscibactin using a SmI2-mediated reformatsky reaction and Zn^{2+}-induced asymmetric thiazolidine formation. Org Lett 16(21):5820–5823
49. De Fuente MC, Segade Y, Valderrama K, Rodríguez J, Jiménez C (2021) Convergent total synthesis of the siderophore piscibactin as its Ga^{3+} complex. Org Lett 23(2):340–345
50. Osorio CR, Rivas AJ, Balado M, Fuentes-Monteverde JC, Rodríguez J, Jiménez C, Lemos ML, Waldor MK (2015) A transmissible plasmid-borne pathogenicity island confers piscibactin biosynthesis in the fish pathogen *Photobacterium damselae* subsp. *Piscicida*. Appl Environ Microbiol 81(17):5867–5879
51. Wang Q, Liu Q, Ma Y, Rui H, Zhang Y (2007) LuxO controls extracellular protease, haemolytic activities and siderophore production in fish pathogen *Vibrio alginolyticus*. J Appl Microbiol 103(5):1525–1534
52. Valderrama K, Balado M, Rey-Varela D, Rodríguez J, Vila-Sanjurjo A, Jiménez C, Lemos ML (2019) Outer membrane protein FrpA, the siderophore piscibactin receptor of *Photobacterium damselae* subsp. *Piscicida*, as a subunit vaccine against photobacteriosis in sole (Solea senegalensis). Fish Shellfish Immunol 94:723–729
53. Lemos Ramos ML, Balado Dacosta M, Jiménez González C, Rodríguez González J, Vila Sanjurjo A, Valderrama Pereira AK. Recombinant ferri-piscibactin receptor protein for vaccination against pasteurelosis in fish. WO2017009511 A1 2017-01-19
54. Valderrama K, Soto-Dávila M, Segovia C, Vásquez I, Dang M, Santander J (2019) *Aeromonas salmonicida* infects Atlantic salmon (*Salmo salar*) erythrocytes. J Fish Dis 42(11):1601–1608
55. Najimi M, Lemos ML, Osorio CR (2008) Identification of siderophore biosynthesis genes essential for growth of *Aeromonas salmonicida* under iron limitation conditions. Appl Environ Microbiol 74(8):2341–2348
56. Balado M, Souto A, Vences A, Careaga VP, Valderrama K, Segade Y, Rodríguez J, Osorio CR, Jiménez C, Lemos ML (2015) Two catechol Siderophores, acinetobactin and amonabactin, are simultaneously produced by *Aeromonas salmonicida* subsp *salmonicida* sharing part of the biosynthetic pathway. ACS Chem Biol 10(12):2850–2860
57. Yamamoto S, Okujo N, Sakakibara Y (1994) Isolation and structure elucidation of acinetobactin., a novel siderophore from *Acinetobacter baumannii*. Arch Microbiol 162 (4):249–254

58. Wuest WM, Sattely ES, Walsh CT (2009) Three siderophores from one bacterial enzymatic assembly line. J Am Chem Soc 131(14):5056–5057
59. Shapiro JA, Wencewicz TA (2016) Acinetobactin isomerization enables adaptive Iron acquisition in *Acinetobacter baumannii* through pH-triggered siderophore swapping. ACS Infect Dis 2(2):157–168
60. Telford JR, Leary JA, Tunstad LMG, Byers BR, Raymond KN (1994) Amonabactin: characterization of a series of siderophores from *Aeromouas hydrophila*. J Am Chem Soc 116 (12):4499–4500
61. Telford JR, Raymond KN (1997) Amonabactin: a family of novel siderophores from a pathogenic bacterium. J Biol Inorg Chem 2(6):750–761
62. Rey-Varela D, Cisneros-Sureda J, Balado M, Rodríguez J, Lemos ML, Jiménez C (2019) The outer membrane protein FstC of *Aeromonas salmonicida* subsp *salmonicida* acts as receptor for amonabactin siderophores and displays a wide ligand plasticity. Structure-activity relationships of synthetic amonabactin analogues. ACS Infect Dis 5(11):1936–1951
63. Balado M, Segade Y, Rey D, Osorio CR, Rodríguez J, Lemos ML, Jiménez C (2017) Identification of the ferric-acinetobactin outer membrane receptor in *Aeromonas salmonicida* subsp *salmonicida* and structure-activity relationships of synthetic acinetobactin analogues. ACS Chem Biol 12(2):479–493
64. Shapiro JA, Wencewicz TA (2017) Structure-function studies of acinetobactin analogs. Metallomics 9(5):463–470